

# Technology Support for High-Throughput Processing of Thin-Film CdTe PV Modules

**Phase I Annual Technical Report  
1 April 1998 — 31 March 1999**

D.H. Rose, R.C. Powell, D. Grecu,  
U. Jayamaha, J.J. Hanak, J. Bohland,  
K. Smigielski, and G.L. Dorer  
*First Solar, L.L.C.*  
*Perrysburg, Ohio*



**NREL**

**National Renewable Energy Laboratory**

1617 Cole Boulevard  
Golden, Colorado 80401-3393

NREL is a U.S. Department of Energy Laboratory  
Operated by Midwest Research Institute • Battelle • Bechtel

Contract No. DE-AC36-98-GO10337

# Technology Support for High-Throughput Processing of Thin-Film CdTe PV Modules

**Phase I Annual Technical Report  
1 April 1998 — 31 March 1999**

D.H. Rose, R.C. Powell, D. Grecu,  
U. Jayamaha, J.J. Hanak, J. Bohland,  
K. Smigielski, and G.L. Dorer  
*First Solar, L.L.C.*  
*Perrysburg, Ohio*

NREL Technical Monitor: H.S. Ullal

Prepared under Subcontract No. ZAK-8-17619-17



**NREL**

**National Renewable Energy Laboratory**

1617 Cole Boulevard  
Golden, Colorado 80401-3393

NREL is a U.S. Department of Energy Laboratory  
Operated by Midwest Research Institute • Battelle • Bechtel

Contract No. DE-AC36-98-GO10337

## NOTICE

This report was prepared as an account of work sponsored by an agency of the United States government. Neither the United States government nor any agency thereof, nor any of their employees, makes any warranty, express or implied, or assumes any legal liability or responsibility for the accuracy, completeness, or usefulness of any information, apparatus, product, or process disclosed, or represents that its use would not infringe privately owned rights. Reference herein to any specific commercial product, process, or service by trade name, trademark, manufacturer, or otherwise does not necessarily constitute or imply its endorsement, recommendation, or favoring by the United States government or any agency thereof. The views and opinions of authors expressed herein do not necessarily state or reflect those of the United States government or any agency thereof.

Available electronically at <http://www.doe.gov/bridge>

Available for a processing fee to U.S. Department of Energy and its contractors, in paper, from:

U.S. Department of Energy  
Office of Scientific and Technical Information  
P.O. Box 62  
Oak Ridge, TN 37831-0062  
phone: 865.576.8401  
fax: 865.576.5728  
email: [reports@adonis.osti.gov](mailto:reports@adonis.osti.gov)

Available for sale to the public, in paper, from:

U.S. Department of Commerce  
National Technical Information Service  
5285 Port Royal Road  
Springfield, VA 22161  
phone: 800.553.6847  
fax: 703.605.6900  
email: [orders@ntis.fedworld.gov](mailto:orders@ntis.fedworld.gov)  
online ordering: <http://www.ntis.gov/ordering.htm>



# Table of Contents

<b>Abstract</b> .....	<b>v</b>
<b>Acknowledgements</b> .....	<b>vii</b>
<b>Preface</b> .....	<b>viii</b>
<b>Introduction</b> .....	<b>ix</b>
<b>1. Equipment, Process, and Fabrication Development</b> .....	<b>1</b>
1.1 Production Experience and Deposition-Equipment Improvement .....	1
1.2 Diagnostics.....	2
1.2.1 Off-line Measurements .....	2
1.2.1.1 CdS Thickness.....	2
1.2.1.2 Pinhole Number Density.....	3
1.2.1.3 Small-cell efficiency on modules.....	3
1.2.1.4 Contactless $V_{oc}$ measurement .....	3
1.2.2 On-line Measurements .....	3
1.2.2.1 Thermal Imaging.....	3
1.2.2.2 CdS Thickness.....	4
1.3 Deposition development .....	4
1.3.1 Uniformity.....	4
1.3.2 Consistency .....	7
1.3.3 Utilization .....	10
1.3.4 Pinholes.....	11
1.3.5 Thin Glass .....	12
1.4 Large-area vapor- $CdCl_2$ system .....	12
1.5 Interconnect process development .....	13
1.6 Module materials and finishing.....	13
1.6.1 Encapsulation with Liquid Polyester Resins.....	13
1.6.2 Tests Performed on Modules and Mini-modules .....	14
1.7 100 MW Coater Design .....	15
<b>2. Efficiency Improvement</b> .....	<b>16</b>
2.1 Small-area experiments.....	16
2.1.1 Thin CdS, buffer layers and TCO treatments .....	16
2.1.1.1 Zinc stannate buffer layer .....	16
2.1.1.2 Sprayed- $SnO_2$ buffer layer .....	17
2.1.2 Improved TCOs.....	18
2.1.3 Post-deposition treatments .....	19
2.1.3.1 Vapor- $CdCl_2$ treatment .....	19
2.1.3.2 Treatment of CdTe with Tellurium Chloride.....	20
2.1.3.3 Plasma cleaning of vapor-chloride-treated samples.....	20
2.2 Large-area experiments.....	20
2.2.1 Defect reduction .....	20
2.2.2 Electrical loss reduction.....	21
2.2.3 Modules.....	21

2.3	Research equipment development .....	22
2.3.1	Large-area sputter deposition system.....	22
2.3.2	Small-area vapor-CdCl <sub>2</sub> system.....	23
2.3.3	Small-area VTD system.....	24
<b>3.</b>	<b>Characterization and Analysis.....</b>	<b>25</b>
3.1	Characterization of films and devices.....	25
3.1.1	Temperature coefficient.....	25
3.1.2	Contactless measurement of V <sub>oc</sub> .....	26
3.1.2.1	Uniformity after CdCl <sub>2</sub> treatment.....	26
3.1.2.2	Effect of Cu on V <sub>oc</sub> .....	26
3.1.3	Photoluminescence studies.....	28
3.1.4	X-ray diffraction.....	30
3.1.5	IV(T).....	30
3.2	Reliability Verification and Improvement.....	30
3.2.1	Accelerated-test, measurement and tracking systems development.....	30
3.2.1.1	Light-soak equipment development.....	30
3.2.1.2	Datalogging for Toledo arrays.....	31
3.2.1.3	Simulator improvements.....	31
3.2.2	Documentation of reliability of devices, modules, and arrays.....	31
3.2.2.1	Outdoor data.....	31
3.2.2.2	Accelerated life tests.....	35
3.2.3	Failure-mechanism research and mitigation.....	36
3.2.3.1	Process variable identification.....	36
3.2.3.2	Contact research.....	37
3.2.3.3	SIMS analysis.....	38
3.2.3.4	Cu-complex research.....	39
3.2.3.5	Cell modeling.....	39
<b>4.</b>	<b>Environmental, Health, and Safety.....</b>	<b>40</b>
4.1	General program.....	40
4.1.1	Emissions survey.....	40
4.2.2	Health monitoring.....	40
4.2	Process and equipment improvements.....	40
4.2.1	Edge delete.....	40
4.2.2	CdS material preparation system.....	41
4.2.3	Waste compactor.....	41
4.2.4	CdCl <sub>2</sub> vapor collection.....	41
4.2.5	Wastewater treatment system.....	41
	<b>Conclusions and future plans.....</b>	<b>42</b>
	<b>Appendix: February 1999 emissions survey.....</b>	<b>43</b>
	<b>Glossary of Abbreviations.....</b>	<b>48</b>
	<b>References.....</b>	<b>49</b>

## List of Figures

Figure 1.1 CdS/CdTe plates produced by pilot-production line .....	1
Figure 1.2 CdS thickness data; a) cross-web profile, b) contour map .....	5
Figure 1.3 Thickness uniformity of large-area thinner-CdS films.....	6
Figure 1.4 Aggregate cross-web CdTe thickness profile.....	7
Figure 1.5 CdTe film thickness for each plate made in the 4 <sup>th</sup> quarter of Phase I.....	8
Figure 1.6 Histogram of Average CdTe thickness per plate for the 1st quarter 1999 .....	9
Figure 1.7 Average CdS thickness per plate during 4 <sup>th</sup> quarter-Phase I.....	9
Figure 1.8 Pinhole number density as a function of cross-web position. ....	11
Figure 1.9 Large-area vapor-CdCl <sub>2</sub> treatment system .....	12
Figure 2.1 Contour plot of efficiencies as a function of two vapor-CdCl <sub>2</sub> variables .....	19
Figure 2.2 Large-area sputter deposition system for research .....	22
Figure 2.3 Small-area vapor-CdCl <sub>2</sub> treatment system .....	23
Figure 2.4 Research VTD system .....	24
Figure 3.1 Contactless-V <sub>oc</sub> as a function of CdTe material removed by lapping .....	27
Figure 3.2 Effects of Cu doping on the PL spectrum in single crystal CdTe .....	28
Figure 3.3 “Aging” effects of Cu-doped CdTe single crystal sample .....	29
Figure 3.4 DC Power of 1kW-nominal First Solar array at NREL in Golden, CO .....	32
Figure 3.5 Accelerated test of “X5” cells (wet CdCl <sub>2</sub> , plus IFL).....	35

## List of Tables

Table 2.1 Cell characteristics for substrates with spray-deposited buffer layers.....	17
Table 2.2 Cell characteristics after light soak at open circuit bias for substrates with spray-deposited buffer layers .....	17
Table 2.3 IV parameters of modules delivered to NREL.....	21
Table 3.1 P <sub>max</sub> T and V <sub>oc</sub> T coefficient calculations from field data.....	25
Table 3.2 Cell characteristics for substrates with and without a ZTO buffer layer .....	36
Table 3.3 IV parameters for mini-modules with standard contacts and all-dry contacts as a function of days light soak.....	37
Table 3.4 Na and Cu levels in stressed cells .....	38

## Abstract

Results and conclusions from Phase I of a three year subcontract are presented. The subcontract, entitled “Technology Support for High-Throughput Processing of Thin-Film CdTe PV Modules”, is First Solar’s portion of the Thin Film Photovoltaic Partnership Program. The research effort of this subcontract is divided into four areas: 1) process and equipment development, 2) efficiency improvement, 3) characterization and analysis, and 4) environmental, health, and safety. During Phase I, First Solar made significant progress in all four areas.

As part of the process development effort, the output of the pilot-production facility was increased. Over 6200 8ft<sup>2</sup> CdS/CdTe plates were produced during Phase I -- more than double the total number produced prior to Phase I. This increase in pilot-production rate was accomplished without a loss in the PV conversion efficiency: the average total-area AM1.5 efficiency of sub-modules produced during the reporting period was 6.4%.

Several measurement techniques, such as large-area measurement of CdS thickness, were developed to aid process improvement. Using these measurement techniques and other experiments, the vapor-transport deposition method was refined. CdTe thickness uniformity and reproducibility were improved and are now satisfactorily controlled: from a population of more than 1100 plates the mean standard deviation within a plate was 7.3% and the standard deviation of individual-plate averages was 6.8%. The CdS thickness has approximately  $\pm 10\%$  variation from the target thickness for 3kÅ layers, but has room for improvement for thin layers. Progress was also made on the interconnect and finishing processes: advanced laser-scribing methods and new encapsulants show promise for reducing costs and improving product quality. And as a final part of this task, two large pieces of equipment were developed. A vapor-CdCl<sub>2</sub> system capable of handling one 8ft<sup>2</sup> plate every 3 minutes was designed and built. A large semiconductor deposition system, called the 100MW coater, capable of producing 1,500,000 8ft<sup>2</sup> CdS/CdTe plates per year, was designed and is under construction. This high-throughput production is made possible by the very high rate of deposition that can be achieved with First Solar’s proprietary vapor transport deposition technique -- the semiconductor layers for an 8ft<sup>2</sup> module will be able to be deposited in 15 seconds.

As part of the efficiency-improvement task, research was done on devices with thin-CdS and buffer layers. A cell with 13.9% efficiency was produced on a high-quality substrate and over 12% efficiency was achieved with a cell with no CdS layer. Various post-deposition treatments, including vapor-CdCl<sub>2</sub>, plasma cleaning, and alternative contacts were investigated and show promise for cost reductions and efficiency improvements. Equipment was also developed as part of the efficiency-improvement task. A large sputter-deposition system was developed to enable buffer-layer and back-contact research on the module scale, a small-area vapor-CdCl<sub>2</sub> system was built to

enable vapor-CdCl<sub>2</sub> optimization, and a small-area vapor-transport system was designed and built to allow research on vapor transport of CdS, CdTe, ZnTe, and other materials.

A number of experiments were performed as part of the characterization and analysis task. The temperature dependence of CdTe modules was investigated; the power output was found to be relatively insensitive (<5%) to temperature in the 25 to 50°C range. The contactless-V<sub>oc</sub> measurement technique was used to determine that vapor-CdCl<sub>2</sub> treatment is more uniform than wet-CdCl<sub>2</sub> treatment. Photoluminescence was used to determine that Cu introduces a shallow acceptor state in CdTe that can be unstable. X-ray diffraction was used to determine that the CdCl<sub>2</sub> treatment results in an increase in the randomization of the crystallite orientation in CdTe films. And finally, current-voltage characterization as a function of temperature was used to investigate a high-voltage breakthrough of the suspected back-contact diode.

As part of the characterization and analysis task, considerable effort was also given to reliability verification and improvement. Because First Solar has had product in the field for periods up to 5 years, significant data exists to help determine whether the modules produced have acceptable long-term performance. The most carefully monitored array, located at the National Renewable Energy Laboratory, was found to have unchanged power output within the margin of error of measurement (5%) after 5 years in the field. Other arrays performed well even under adverse conditions. The output of one array was found to be decreasing at approximately 2%/year, but measurements of individual modules showed the average of individual modules to be essentially unchanged. Other arrays showed some loss in individual modules. Considerable effort was also spent on developing accelerated life tests and using light soaking as an accelerated life test. The first round of National CdTe Team stability tests were concluded. One back-contact formulation resulted in cells that increased in efficiency as a result of 9700 hours of light soaking. Cell modeling was also done which highlighted the importance of understanding how back contact treatments can affect device open-circuit voltage. Given the importance of field stability, it was determined that continued monitoring of field data, research on stress-induced-change mechanisms, and accelerated-test development will remain top priorities.

As part of the environmental, health, and safety task, an emissions survey was performed for the pilot-production facility. For production of 360 modules/day it was predicted that the cadmium emissions would be only 0.015% of the level that would require any permitting; however, methanol emissions may require permitting if anticipated process changes are not implemented. Process improvements in edge delete, CdS material preparation, waste compaction, CdCl<sub>2</sub>-vapor collection and wastewater treatment were made, resulting in reduced costs, reduced emissions, and improved operator safety.



## Acknowledgements

We gratefully acknowledge the contributions of the following members of the First Solar Team:

Technical: John Bohland, Eugene Bykov, John Christiansen, Todd Coleman, Todd Dapkus, Gary Dorer, Matt Flis, Andy Gray, Dan Grecu, Joe Hanak, Rick Harju, Upali Jayamaha, Linda McFaul, Harold McMaster, Rick Powell, Nick Reiter, Geoff Rich, Scott Roberts, Doug Rose, Ken Smigielski, Mike Steele

Equipment development: Leo Adoline, Gary Faykosh, Jim Foote, Jim Hinkle, Terry Kahle, Jeff Klopping, Ken Kormanyos, Alan McMaster, Bob Notestine, Jim Poddany, Dene Rinaldo, Mike Ross, Darrel Wirebaugh

Production: Dave Berger, Tony Biddle, Verlin Champion, Stan Collins, Steve Cox, Tim Foreman, Antonio Garcia, Rebecca Higbea, Richard Hurtado, Jeff Hutton, Racquel Jaros, Len Lawniczak, Roger Long, Mike McArthur, Brian McMullen, Kevin Miller, Russell Norris, Kirk Papenfuss, Beth Reese, Terry Seeman, Larry Thornton, Robert Wurzelbacher

Support and management: Phyllis Allman, Don Baldwin, Larry Crosser, Larry Cicak, Greg Darr, Ruthie Foore, Mike Hayes, Joy Jaqua, Jim Jaros, Steve Johnson, George Khouri, Greg Nelson, Judy Pollack, Angela Reidling, Tracy Ross

We are also grateful to Sally Asher and Matt Young of NREL for SIMS analysis, Harin Ullal, Ken Zweibel, and Bolko von Roedern of NREL for technical and contract guidance, Tim Gessert and Xuanzhi Wu of NREL for ongoing collaboration, Ben Kroposki of NREL for array measurement, Halden Field of NREL for assistance with simulator improvement, Dave King of Sandia National Laboratory for array measurement, Neelkanth Dhere of FSEC for module measurement, and all of the other members of the National CdTe Team for ongoing collaborations and discussion.

This work has been supported in part by NREL subcontract ZAK-8-17619-17.

## Preface

This report is the first annual report for a subcontract awarded to Solar Cells, Inc. (SCI) in 1998. SCI had been conducting research and process development on CdS/CdTe solar panels since 1991. In February 1999, SCI and True North Partners, LLC of Phoenix, Arizona jointly formed First Solar, LLC. True North Partners is a private equity firm which participates with selected companies by providing capital and operating experience. First Solar assumed all activities of SCI, including the research described in this report.

The vision of Solar Cells, Inc. had been to produce photovoltaics at costs competitive with traditional energy sources. Part of that vision was to develop processes for manufacturing of photovoltaics (PV) such that incorporation of a conventional glass-processing line would be possible. A typical float-glass line produces 600 tons of glass a day, which if used for 10%-efficient modules using a 3mm-thick front glass and 2mm-thick back glass, would in one year produce photovoltaic panels with over 1GW peak output. Thus, 1 plant could produce over 5 times the current world PV production. First Solar has retained the goal of very high-throughput production, but has accelerated the time-line for the development of a medium-scale (20 to 100MW) production facility. This facility is currently under construction in Perrysburg Township, OH.

First Solar has several advantages which make the realization of the goal of high-throughput, inexpensive photovoltaics possible. First, the company has developed processes amenable to high-throughput production: the proprietary, vapor-transport deposition process enables deposition of the critical semiconductor layers on a 2ft x 4ft module in less than 30 seconds. Second, the processes developed produce high quality panels at a low cost. Third, the company has tremendous expertise in the handling of glass at high temperature - the importance of this knowledge was key to the decision to locate SCI in the "Glass City", Toledo, OH, in 1991. And fourth, the company now has the financial backing to move rapidly into the production phase. The excellent position of the company is due to support from its shareholders, the U.S. Department of Energy, the National Renewable Energy Laboratory, its constituents and partners, as well as the energy and efforts of its employees and the efforts and vision of SCI's founder, Harold McMaster.

## Introduction

CdTe has long been recognized as possessing near-ideal properties for the conversion of solar energy [1]. The energy gap is near optimum for a single junction solar cell [2], the high absorption coefficient allows films as thin as 2  $\mu\text{m}$  to absorb more than 98% of the above-bandgap light, and cells with efficiencies near 16% have been produced [3, 4]. The desirable properties of CdTe also extend beyond those useful for the production of small-area laboratory cells -- the simplicity of the binary CdTe system and the remarkable ability of CdTe to compensate for defects suggest that CdTe deposition for solar panels is amenable to robust manufacturing processes. The suitability of CdTe for high-volume, low-cost manufacturing of solar panels is supported by the large number of deposition techniques that have been used to produce cells with efficiency greater than 11% [5]. Furthermore, stability of the CdS/CdTe junction has been demonstrated [6, 7] and the health and safety concerns of cadmium, including recycling, have been shown to be manageable in a cost-effective and responsible manner for both manufacturing and product deployment [8-11].

First Solar has been the leading developer of high-speed, thin-film deposition techniques for CdTe photovoltaic modules. Using a proprietary vapor-transport deposition technique developed at Solar Cells, Inc (now First Solar), the semiconductor films for an 8ft<sup>2</sup> module can be deposited in less than 30 seconds [12]. First Solar has also developed reasonably high-throughput processes for the remainder of the steps required to make finished modules and has been producing modules in various levels of pilot production for 5 years. Modules with power output up to 60.5 W under standard conditions have been produced (area of 0.72m<sup>2</sup>) and field stability has been demonstrated [6].

The goal of the Thin-Film Photovoltaic Partnership program is to advance the state-of-the-art of large-scale thin-film module fabrication. The subcontract awarded to First Solar as part of the program leverages First Solar's extensive knowledge and equipment base to achieve that goal. The subcontract is divided into four areas of effort: i) process and equipment development, ii) efficiency improvement, iii) characterization and analysis, and iv) environmental, health, and safety. During Phase I, First Solar made significant progress in all four areas.

This report is organized in the same manner as the task description of the subcontract, with the exceptions that Task 3.5 of the statement of work (Research VTD chamber design) is reported in section 2.3.2 of this report, and Task 3.6 (Zn<sub>2</sub>SnO<sub>4</sub> research) is reported in section 2.1.1.

# **1. Equipment, Process, and Fabrication Development**

## **1.1 Production Experience and Deposition-Equipment Improvement**

Work continued on the development of the vapor-transport deposition (VTD) method during Phase I. The pilot equipment produced nearly 6600 plates (60 cm x 120 cm) during this time period. Approximately 5% of these plates were CdS-only depositions. 2700 of the bi-layer (CdS/CdTe) plates were processed into active sub-modules. Many of the sub-modules were finished into packaged modules and sold. In addition, many of the coated plates were sold directly to customers. The number of plates produced during Phase I was more than double the total number produced prior to Phase I (see Figure 1.1). The number of sub-modules produced during Phase I was 15% higher than the total number of sub-modules produced prior to Phase I. As a result, we gained a lot of experience with the deposition system. The primary VTD components performed very well. The incidence of breakage and chemical corrosion was minimal. Occasional clogging in the material supply lines was encountered, but the frequency was not excessive.

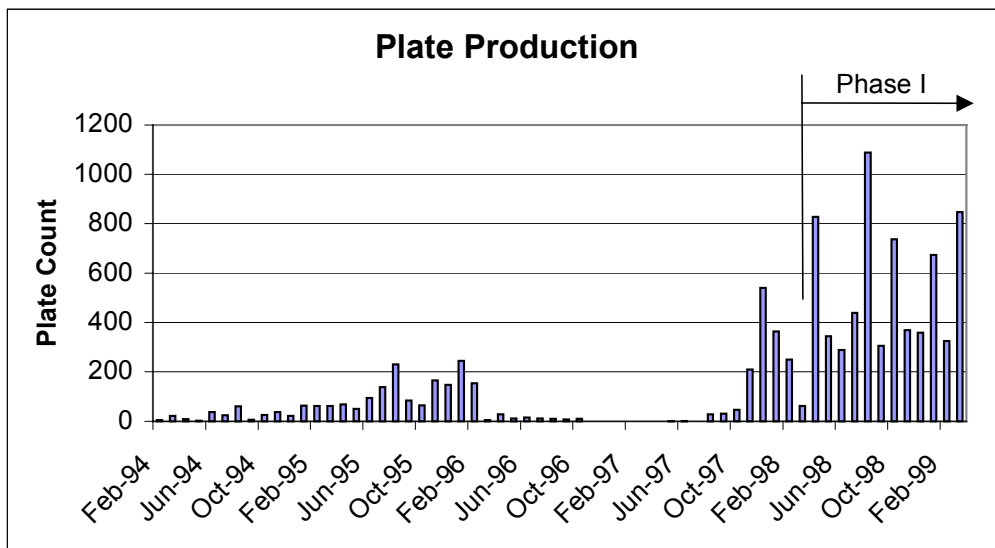


**Figure 1.1** CdS/CdTe plates produced by pilot-production line

The average aperture efficiency of the sub-modules made during Phase I was 6.8% (6.4% total-area efficiency). In aggregate, these performance numbers are virtually identical to the experience prior to Phase I. Thus the increased volume did not result in a loss of performance.

Several modifications were made to the pilot-production line VTD system during phase I. These modifications were made to reduce system down-time, improve deposition quality, and increase space in the system to allow testing of new vapor distributor concepts. One of the modifications to the deposition system was the installation of a new external exhaust system. Four tubes exiting the VTD-system side walls were piped through a

cooling unit and then through a large filter. Prior to the cooling unit, all joints were sealed with metal gaskets. The new exhaust system, which included new and larger throttle valves, resulted in a marked improvement in the management of gas flow within the coating chamber and was capable of maintaining VTD system pressures at higher gas flows.

New problems resulting from the increased usage of the system were solved as they arose. For example, an episode of non-uniformity of the CdS film was traced to a gas leak in one of the supply lines; in response, the fittings were upgraded and the alarm levels on the back-pressure sensors were adjusted to be more sensitive. To further reduce down time a trouble-shooting guide for the VTD system was assembled. This guide summarizes many of the standard procedures developed previously for diagnosing coating problems.

## **1.2 Diagnostics**

A significant amount of effort was expended in developing several automated measurement techniques that permit spatial mapping of film characteristics. We envision a combination of on-line and off-line inspection methods for the production line. Typically, techniques are developed in an off-line mode then are considered for on-line implementation. In the following sections each technique will be briefly described. Examples of resulting data will be presented in the subsequent sections describing process development.

### **1.2.1 Off-line Measurements**

A number of off-line measurement techniques were implemented on an automated, full-module X-Y motion system. Using fixed-position excitation/detector pairs, the X-Y movement enables high-density mapping of several important quantities. Sampling every centimeter produces excellent maps and is used for research experiments but several hours are required for a complete measurement. As a quality-control tool, sampling every 2 centimeters is adequate. The first two mapping measurements to be implemented were CdS thickness and pinhole density. Work continues on components to measure CdTe thickness and  $V_{oc}$  on partially processed films. Functionally each measurement is treated as a generic transducer and thus all of these systems share the same control and data handling system. Data can be displayed as color maps, contour plots or as averaged cross-web or down-web profiles.

#### **1.2.1.1 CdS Thickness**

CdS thickness is inferred from a simple, single-wavelength optical transmission measurement. The system employs a modulated blue LED, a Si PIN photodiode, and a lock-in amplifier. No correction is made for reflection variations. Compared to the beta-backscatter technique currently used to measure film thickness in production, this technique is vastly superior.

#### 1.2.1.2 Pinhole Number Density

Pinholes are a continuing concern particularly in a high-throughput thin-film deposition system. Prior to Phase I only qualitative information existed about pinhole number densities present in films; consequently, only dramatic differences could be discerned. Therefore we constructed a system to count pinholes automatically. The primary components of the system are a light source, a CCD camera, and a frame grabber. Software routines available with the frame grabber perform the digital signal processing required to delineate and count features in the pixel image.

#### 1.2.1.3 Small-cell efficiency on modules

The capability to measure 1-cm<sup>2</sup> 'dot' cells was set up temporarily on the large vertical X-Y table. A set of probes and cables was assembled so that cell IV measurements can be made using the computer system from the large simulator but with the module positioned on the large vertical X-Y table and the cell illuminated with the W-filament back-light. This technique has 2 advantages. First, the plate temperature doesn't increase in the time between first cell and last cell measurement. Second, each cell is illuminated with the same light source and for the same period of time, unlike when the cells were measured on the large simulator. Thus, accurate comparison of photocurrents between cells can be made with assurance that any differences in the results are not due to variations in the light intensity.

#### 1.2.1.4 Contactless $V_{oc}$ measurement

In the Phase III program it was reported that the open-circuit voltage ( $V_{oc}$ ) of SnO<sub>2</sub>/CdS/CdTe films could be measured by making a temporary contact to the CdTe back surface with a graphite foam pad. Accurate readings could be obtained in less than 2 seconds, making this technique well-suited for mapping of  $V_{oc}$  over substrates having large areas. Therefore it was decided to adapt the  $V_{oc}$  detector to the large X-Y vertical scanning table which already has thickness and pinhole measurement capabilities. A new  $V_{oc}$  detector was built for this purpose. The output from the  $V_{oc}$  detector is relayed to the data acquisition system of the lock-in amplifier so the readings can be obtained under computer control. An electrically operated solenoid with a graphite foam tip was installed to make a temporary contact. A 39-W quartz halogen lamp was used to illuminate the sample. As a ripple-free illumination is required, the lamp is powered by a DC power supply.

Preliminary results indicate that stable readings could be obtained in about one second which is comparable to the time taken for a thickness measurement. Integration of this contactless  $V_{oc}$  measurement system to the X-Y scanning program was attempted, so that maps of  $V_{oc}$  could be generated over the entire area of the coated substrates. It was found, however, that the graphite foam picks up fine particulates, thus making the readings unreliable. Work is continuing in an effort to improve the procedure.

### **1.2.2 On-line Measurements**

#### 1.2.2.1 Thermal Imaging

During Phase I we installed a commercial, on-line thermal imaging system capable of viewing the glass within the deposition vacuum system. The initial thermal maps

suggested that the glass edges were significantly hotter than the central region. However, after additional investigation, we believe that the TCO layer causes significant artifacts in the data. Thermal images from clear glass indicate that the glass edges are only slightly hotter. Nevertheless, several recurring film features correspond with the original thermal maps and thus work with the IR scanner continues.

#### 1.2.2.2 CdS Thickness

Work began on adapting the optical absorption technique, which is successfully used in the off-line mode for in-situ measurement of the CdS film thickness. The adaptation includes the use of a green laser rather than a blue LED since higher power is required on account of the much longer optical path and the desire to avoid lock-in detection. Moreover, since the measurement will occur at deposition temperatures, significant bandgap narrowing permits the use of longer wavelength light sources.

### **1.3 Deposition development**

#### **1.3.1 Uniformity**

Several measures have been used to ascertain the film uniformity. Foremost is thickness uniformity. Typically achieving cross-web uniformity presents a greater challenge than attaining down-web uniformity. Furthermore, we believe that the thickness uniformity of CdS is more important than that of CdTe. Figure 1.2 shows a contour plot of CdS thickness of a standard production CdS-only film. Except for several extreme edge locations, the thickness uniformity is within  $\pm 10\%$  of the target thickness of 3.0 kÅ.

Our goal, however, is to produce much thinner CdS films with more stringent uniformity constraints. Figure 1.3 shows the best attempt to date of thin CdS formed using production-scale VTD. A contour plot map of one plate is shown along with average cross-web profiles taken from 3 pieces produced on the same day. The 2 humps in the cross-web profile are remnants from the source material introduction from either side.

CdTe thickness uniformity was assessed using thickness data obtained from the beta-backscatter system. The beta-backscatter thickness measurement is currently taken at 13 locations on every production plate. Figure 1.4 shows aggregate cross-web averages for all CdTe plates made during the 4<sup>th</sup> quarter of Phase I. From this data we can conclude that CdTe uniformity is more than adequate for our needs.

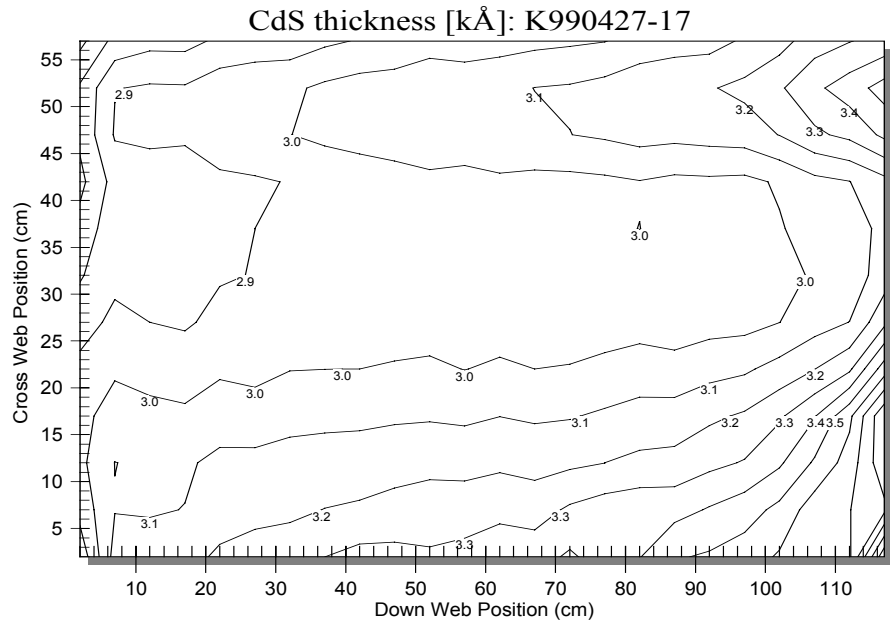
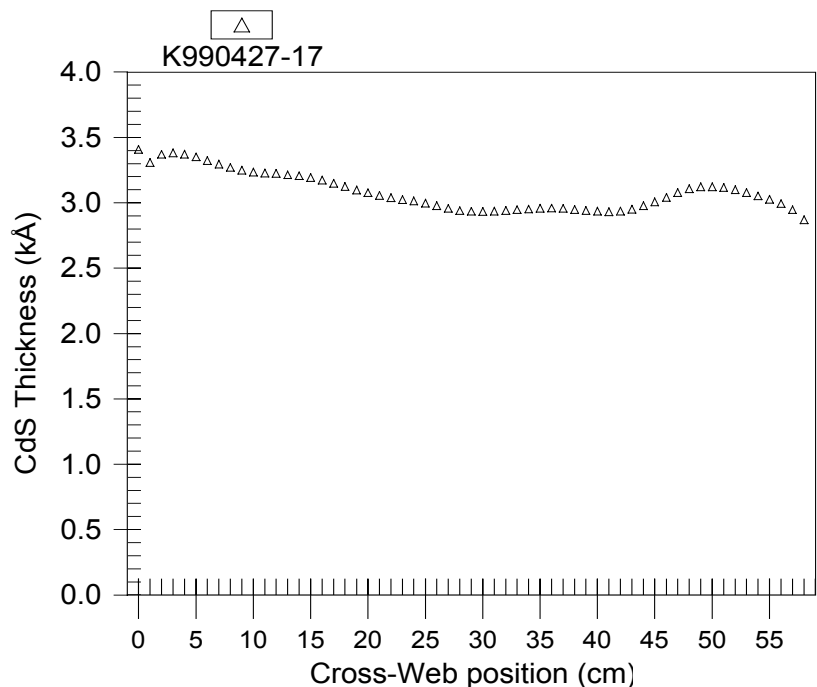


**Figure 1.2** CdS thickness data derived from optical transmission data; plate produced with baseline production settings with a target CdS thickness of 3 kÅ. a) Average cross-web profile, b) Contour map.



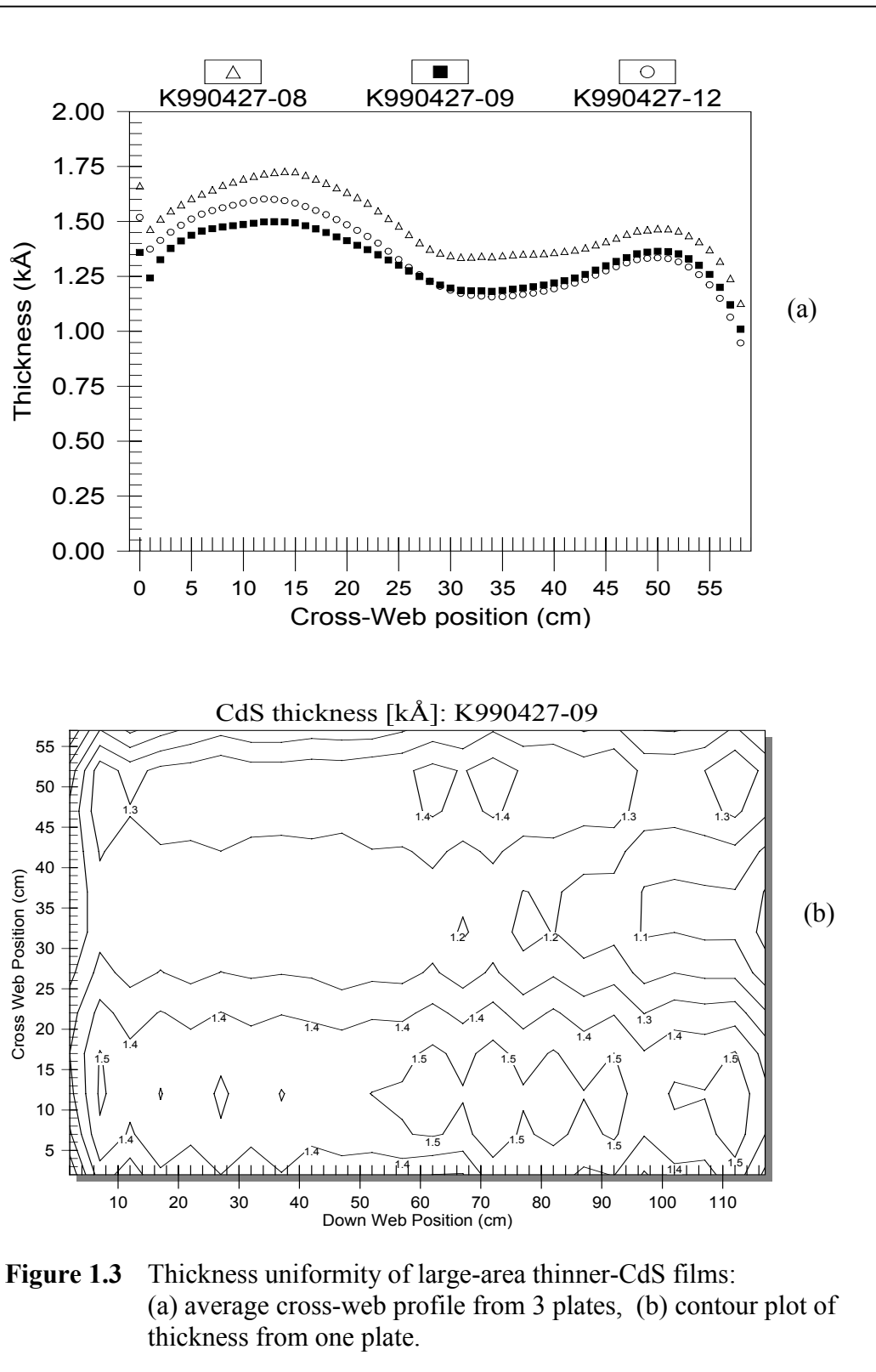


**Figure 1.3** Thickness uniformity of large-area thinner-CdS films: (a) average cross-web profile from 3 plates, (b) contour plot of thickness from one plate.

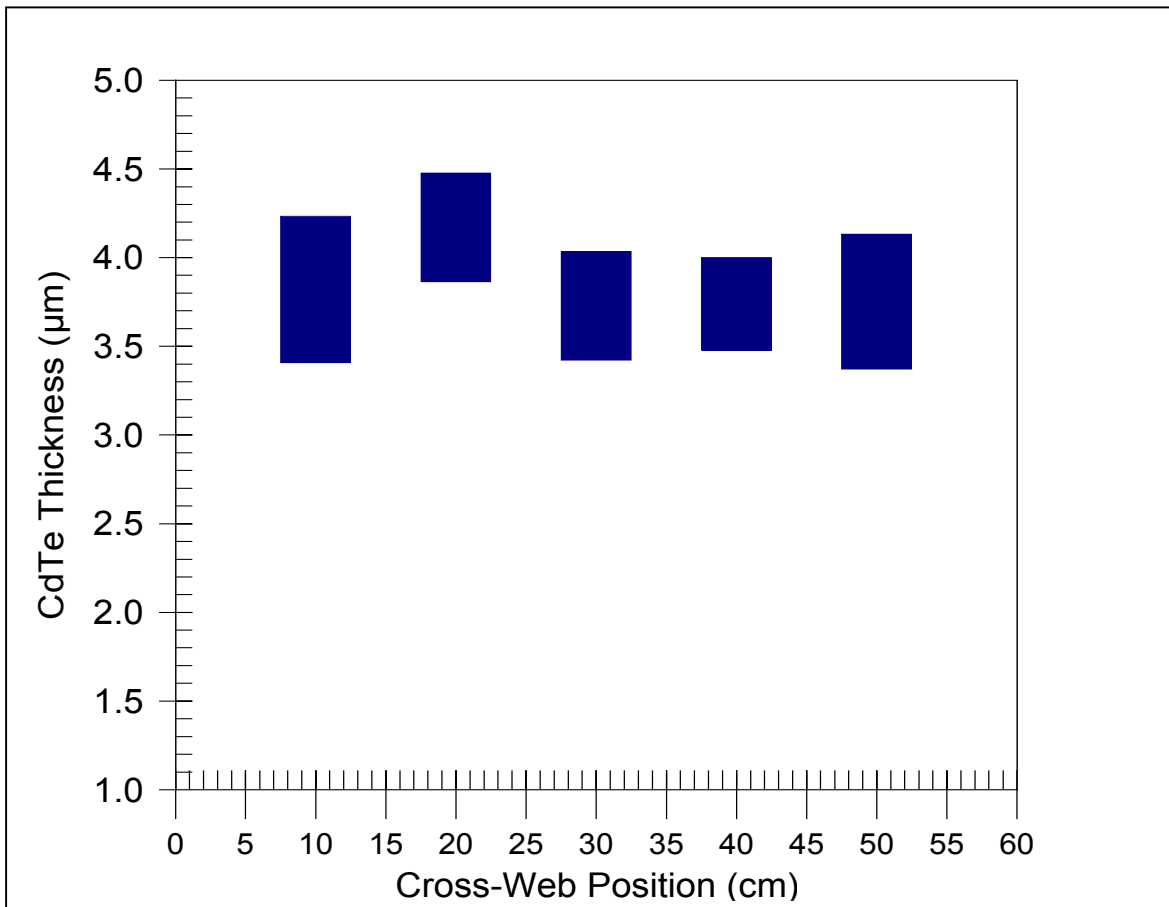


**Figure 1.4** Aggregate cross-web CdTe thickness profile derived from beta-backscatter measurements. Data is averaged from all plates made during the last quarter of Phase I. Boxes represent averages  $\pm$  1 standard deviation.

### 1.3.2 Consistency

The ability to deposit high-quality films consistently is obviously important. To assess this capability, we first examine the film thickness data. We use the statistics of the 13 beta-backscatter measurements taken on every plate as a metric. Figure 1.5 shows the average and standard deviation of the CdTe film thickness for each plate made in the 4<sup>th</sup> quarter of Phase I. Figure 1.6 is the same data displayed as a histogram. This data demonstrates the production capability of the system.

Similarly we can examine the CdS data. In production, CdS film thickness is sampled off-line with a frequency of about 5% using beta-backscatter. Figure 1.7 shows the average CdS thickness per plate made during the 4<sup>th</sup> quarter of phase I. All sampled plates are shown including those made while adjusting CdS to the target thickness; consequently the data is severely biased. The inadequacies of this current method highlight the need for our ongoing work developing an in-situ CdS thickness sensor.

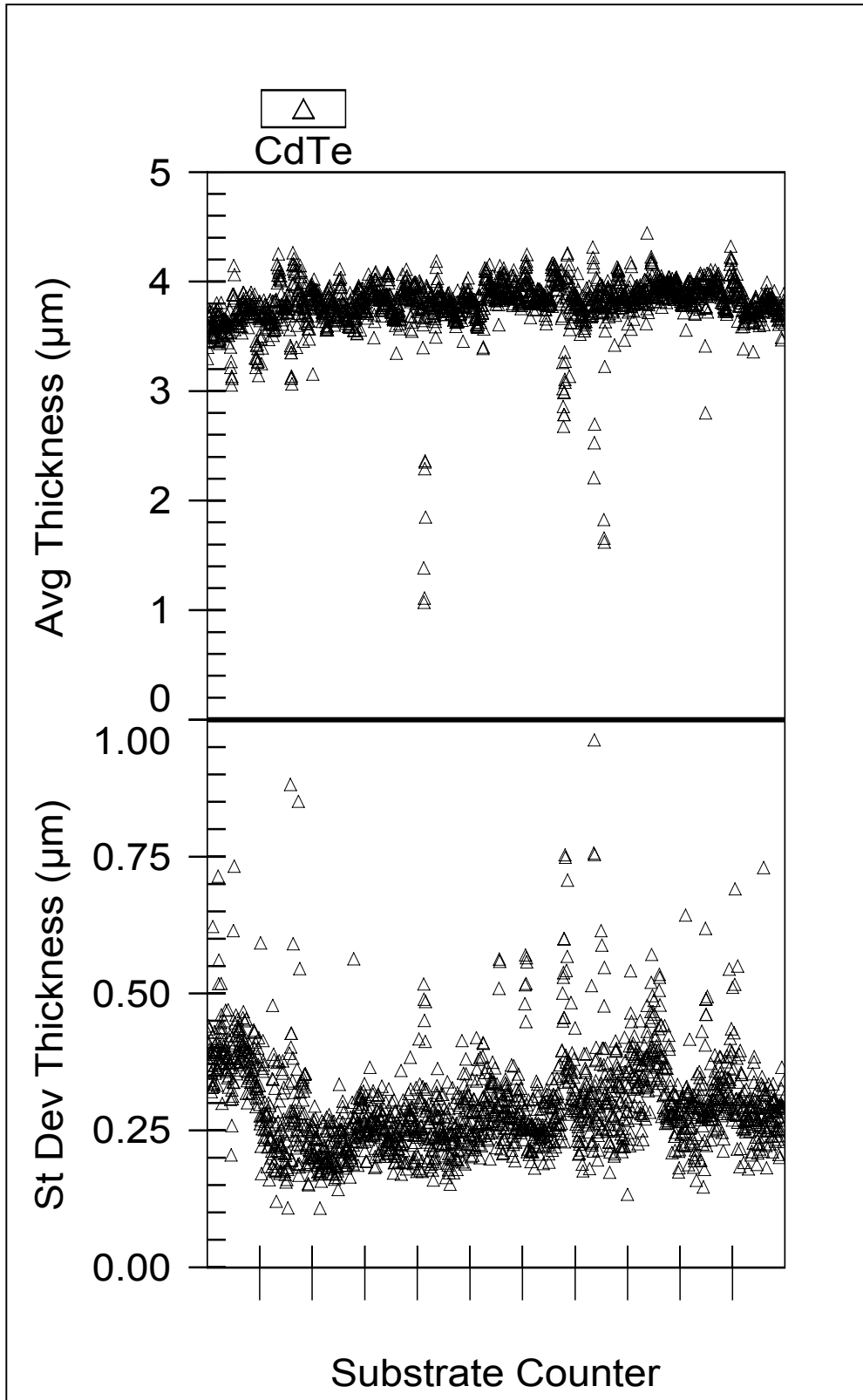
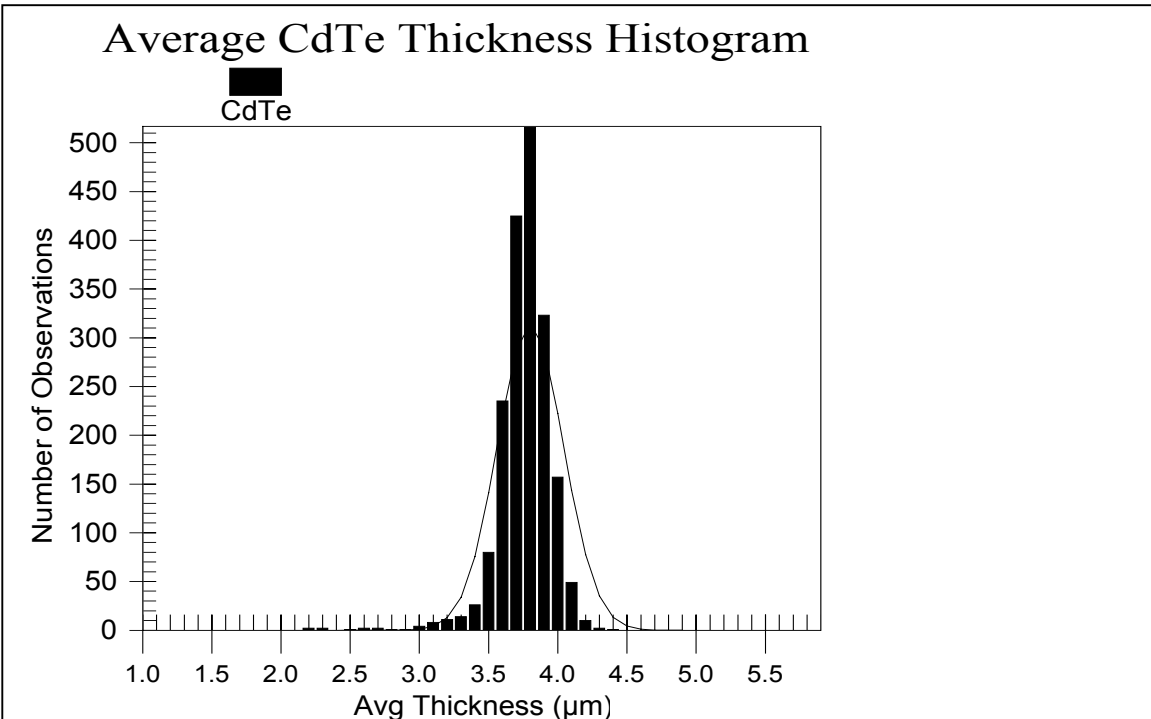
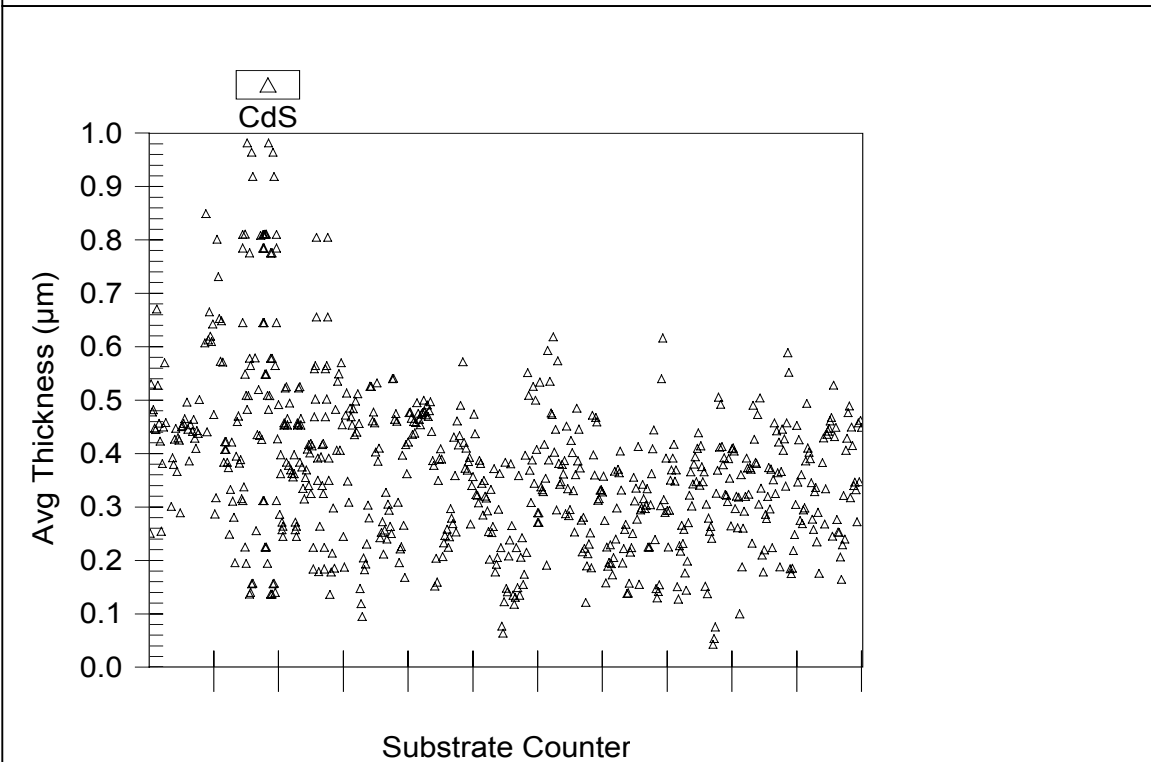


Figure 1.5 CdTe film thickness for each plate made in the 4<sup>th</sup> quarter of Phase I



**Figure 1.6** Histogram of Average CdTe thickness per plate for the 1st quarter 1999. Average thickness per plate is derived from a 13 point sampling using a beta-backscatter detector.



**Figure 1.7** Average CdS thickness per plate during 4<sup>th</sup> quarter-Phase I. All sampled films are shown including many that were used to adjust CdS settings.

### 1.3.3 Utilization

High material utilization of costly semiconductor source material is important for low-cost and low-maintenance production. During Phase I we produced a significant number of plates and monitored our usage more closely than in the past. In the current pilot deposition equipment, a discontinuous stream of glass plates moves through the system. The source material flow is interrupted whenever substrates are not present in the deposition zone. Since some time is needed to establish steady-state, the material flow is initiated prior to the arrival of the next piece. Because this mode will not be used in the production equipment, we have corrected the gross-utilization.

The corrected CdTe material utilization experienced with the pilot equipment was 72%. This estimated utilization is short of the target goal (80% for an 8 hour run), but remains promising. Our original estimates for ultimate material usage were based largely on the demonstrated excellent start/stop and side definition growth patterns demonstrated previously [12]. Two CdTe utilization loss mechanisms that we have identified are “web-edge overspray” and re-sublimation. Currently we err on the safe side for uniformity and accept the overspray; the overspray results in coating on the sunny-side which then must be removed. Re-sublimation of CdTe occurs after deposition while the film/glass remains hot and in vacuum. A non-negligible loss of 10% or greater can occur, with the leading edge affected more. In the future, we believe improved glass handling will allow us to lower the glass temperature sooner, greatly reducing this loss.

For CdS, the corrected material utilization was found to be 29%. The first CdS loss pathway occurs prior to material introduction into the chamber. Our current CdS vendor supplies us with an extremely fine CdS powder that is unusable as-received. We have developed an additional process step that converts the as-received CdS into an easy-to-handle form. However, yields for this process have varied widely, between 50 and 90%. The second CdS loss path is the overspray mechanism discussed above. However, we do not believe that these losses are sufficient to account completely for the utilization deficit.

We believe that details in the CdS growth kinetics contribute to the low utilization. The net incorporation probability of incident Cd and  $S_x$  vapor species is controlled by residence time on the surface and the sequence of bond re-arrangement that leads to compound formation and thus film growth. Low adsorption energies, which are likely, result in short residence times before desorption. Since VTD is a high-rate technique that may not confine the vapors well, desorbed fluxes are probably lost. Furthermore, incident polyatomic  $S_x$  species ( $x = 2$  to 8) require adsorption and dissociation prior to incorporation. These same mechanisms are operative during CdTe deposition as well but apparently are not as severe in our VTD implementation. Researchers at the Institute of Energy Conversion report that in their physical vapor deposition system, apparent sticking probabilities for CdTe depositions drop to 10% when substrate temperatures were increased from 275 to 350°C. One possible solution is to supply excess S to the growth ambient; this work will be part of an SBIR Phase II award and initial experiments have shown some promise. Of course, reducing the CdS layer thickness, which is part of the ongoing effort to raise module efficiency, would also reduce the amount of CdS used.

### 1.3.4 Pinholes

Using the automated pinhole counting apparatus described in section 1.2.1.2, we began to map the pinhole number density present in production films. Figure 1.8 shows average pinhole counts as a function of cross-web position for several recent films. We consistently observe significantly higher pinhole number densities near the web edges and usually the profile is quite asymmetric, e.g. sample K990329-19 in Figure 1.8. Based on past qualitative observations, many of the current production films have significantly greater pinhole counts. Thus we have made better films in the past. Moreover, the pinhole number density is quite low in the web center, hence the presence of pinholes is not inherent to the VTD process. We believe that the source of most of the pinholes is CdS particulates. These particulates derive primarily from incomplete vaporization, which in turn is a result of deficient thermal geometry. The location of the greatest pinhole number density occurs on the side of the deposition equipment where the carrier

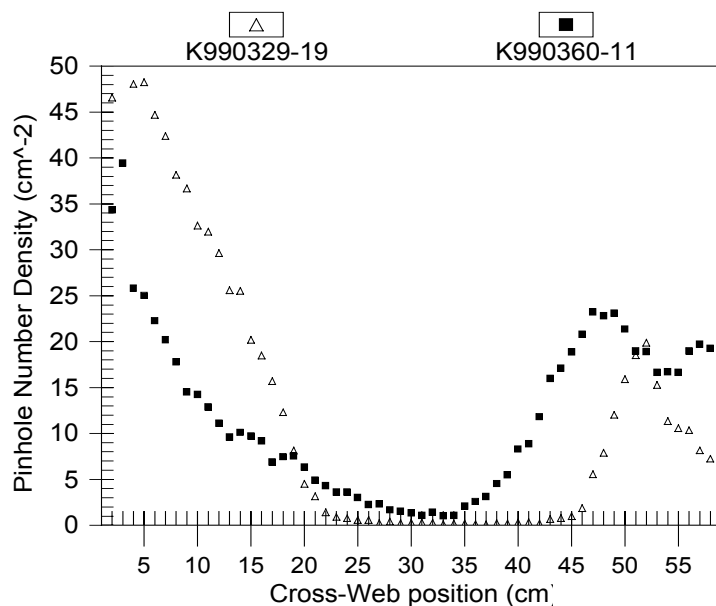


**Figure 1.8** Pinhole number density as a function of cross-web position. Data was derived from 2 dimensional sampling, which was then averaged in one dimension. High densities near the web edge are caused by thermal geometry.

gas pre-heat is the least effective (the chamber is asymmetric). Consequently, we are confident that simple improvements in the thermal profile will significantly decrease the pinhole density near the web-edges. Curiously while some locations have significant pinhole numbers, we have not found an expected efficiency loss in these regions. This is partly due to subsequent device processing. Nevertheless, a reduction in pinhole formation will be forthcoming.

### 1.3.5 Thin Glass

Prior to Phase I, the type of substrate used was 60-cm wide, 120-cm long and 5-mm thick glass plates. Since a reduction in the thickness of the glass would enable substantial cost savings, a transition to 3-mm thick glass was attempted with favorable results. Because of faster heating, the 3-mm thick substrates were transported at a speed of 2.0 m/min. (6.7 ft/min.), compared with 1.38 m/min. (4.5 ft/min.) for the 5-mm substrates. To attain the required semiconductor film thicknesses, the source feed rates were increased and flows adjusted until uniformity was achieved. In addition, 2.3-mm thick glass substrates were successfully coated at a linear speed of 2.3 m/min. (9 ft/min.). The films were qualified as dot cells and full modules. This rate corresponds to more than 1,000,000 60cm x 120cm plates per year, or about 60 MW<sub>p</sub> for 8%-efficient modules. Thus the thinner glass can also reduce production costs because of increased throughput.

### 1.4 Large-area vapor-CdCl<sub>2</sub> system

During Phase I we completed the design and construction of a full-scale vapor-CdCl<sub>2</sub> treatment system capable of handling the throughput of the pilot deposition equipment. The equipment was located immediately downstream from the pilot deposition system thereby eliminating the glass heating prior to chloride treatment. In fact, after quenching, the glass exits the deposition chamber within 50°C of the temperature needed for chloride treatment. The new system provides for treatment duration up to 15 minutes with a throughput of up to one 60cm x 120cm plate every 3 minutes. Testing of the vapor generators and pilot-line implementation of the overall dry chloride treatment will commence during the first half of Phase II. The system is shown in Figure 1.9.



**Figure 1.9** Large-area vapor-CdCl<sub>2</sub> treatment system

## **1.5 Interconnect process development**

Cell patterning and interconnect using reliable, low-cost processes is important to the achievement of high-throughput, inexpensive solar panels. During Phase I we worked both on the exploration of new higher-throughput laser-scribing approaches and on increasing the understanding of laser scribing of our material.

One alternative for high-throughput processes, the use of many lasers, was made possible with the recent advances in diode-pumped laser technology. More than a dozen companies were identified and contacted that indicate capabilities in high-power diode-pumped lasers. In addition, First Solar technical staff attended the industrial laser exhibit in Chicago and visited laser vendors. Concepts such as laser-beam splitting and cylindrical optics were also explored to further reduce total-system costs.

Another alternative considered was a continuous laser. A series of scribing experiments was conducted in continuous (CW) and pulsed mode on the ILM system (motion table by ILM of Columbus, OH) that generates a low infrared laser beam of 1064 nm. The purpose was to reproduce the results obtained with a diode-pumped CW 'FiberLaser' from DLS and to compare results of CW and pulsed laser scribing. It was found that for the CW mode the ILM had insufficient power to achieve scribe-1, however, in the pulsed mode, scribe-1 could be achieved even at high line speeds of 300 in/min. Because of the combination of the high cost of the CW Fiber laser (\$3.5 M per system) and superior results with Q-switched lasers, the use of CW lasers was not pursued further.

The tradeoffs involved in the various wavelengths of lasers was also explored. It was demonstrated that infrared laser radiation (non-frequency doubled YAG laser radiation) was capable of producing high-quality scribes 1, 2, and 3. The laser used was a lamp-pumped Nd:YAG having a pulse width of several hundred ns; the shorter pulse widths available with diode-pumped lasers should make scribe-3 even easier to accomplish. A new T30BL6-532Q laser from Spectra Physics was also evaluated. The laser is capable of both high quality green 532 nm in excess of 3 watts and infrared 1064 nm in excess of 5 watts. The short pulse width (~10 ns) and high pulse frequency (up to 100 kHz) and long life (>10,000 h) could provide quality and cost benefits in the scribing process.

## **1.6 Module materials and finishing**

A significant item in the cost reduction of high-throughput manufacture of PV modules is final encapsulation, which currently utilizes EVA. A liquid polyester resin is a candidate material that may meet the expectations of low cost of unit assembly and product longevity. Styrene-based polyester resin systems are already used worldwide in architectural glass laminating applications and aliphatic-based resins are used in extremely challenging environmental conditions.

### **1.6.1 Encapsulation with Liquid Polyester Resins**

Two resin systems are available for glass lamination, however, neither of them has been tested for PV applications. Because of the low cost and already proven applications elsewhere, an exploratory program of investigating these materials for rear encapsulation



of CdTe PV modules was undertaken. The two systems tested were the Zircon system and the Glasslam System; the former turned out to be preferable because it contains no unbound plasticizers. The liquid resin, to which a catalyst and an adhesion promoter are admixed just before use, is poured in between the module and the cover glass. Narrow tape, of desired laminate thickness, is used both as a spacer and as sealant around the edges between the two plates. The resin can be cured in as little as 7 minutes in a low temperature infra-red oven.

### **1.6.2 Tests Performed on Modules and Mini-modules**

A limited number of 60cm x 120cm modules and 10cm x 10cm mini-modules have been fabricated and tested. A visual comparison of the polyester resin lamination with EVA (ethylene vinyl acetate) lamination showed the quality to be similar, with no air bubbles present. The conversion efficiency did not change significantly upon lamination. All modules have passed the MQT hi-pot test and one has passed 20 cycles of heat-humidity-freeze cycling (MQT requires only 10 cycles).

The module that passed the heat-humidity-freeze test has been also subjected to “damp heat” test (1,000 hours at 85% humidity and 85°C). The module failed this test. It failed the hi-pot test and was visibly delaminated in all corners, perhaps 1 or 2% total delamination area. This was one of the first modules made using this lamination process. This resin was manufactured by the Glasslam system which uses plasticizers which provide reduced adhesion to the glass. By comparison, a module laminated with EVA in an autoclave initially failed the hi-pot test after heat-humidity-freeze cycling. However, it did not delaminate after the damp-heat test. It showed more bus bar corrosion than the polyester resin module. The module laminated with EVA showed a white haziness in the edge deletion area, while the module laminated with polyester resin showed a slight yellowing at the edges.

More promising stress test results (pressure cooker and high exposure UV testing) were obtained with the Zircon system on small samples. Small scale testing using an electric pressure cooker was completed on glass-to-glass laminated samples to compare these encapsulant systems exposed to steam at 15 PSI. Again, the EVA showed distinct white haziness, worse at the edges but progressing nearly to the sample center, while the polyester samples showed a slight yellowing. Neither system showed delamination.

A stress test using high intensity UV irradiation provided by the F300 Fusion UV curing system showed interesting results. The total irradiance between wavelengths of 200 and 600 nm, with a maximum at 380 nm, was 139.6 mW/cm<sup>2</sup>. Polyester polymers, not noted for resistance to UV energy, fared no worse than the EVA, possibly because of the presence of antioxidants and UV blockers added to the resin formulation. In the first 72 hour exposure test, both EVA and polyester test pieces (laminated using quartz for the cover glass) had an increase in optical density to a value of 0.06 at the test conclusion. The EVA turned brownish while the polyester became yellow; the respective yellowing indices were 35 and 48. Adhesion testing performed at the University of Toledo with a calibrated press done after the 72-hour UV exposure showed no change in the shear force

to failure for the polymer, however, it produced a decrease down to 38% for the EVA lamination.

Mini-modules were also exposed to high intensity UV light through the rear glass cover, which for this test was fused silica. Three PV devices, encapsulated with EVA and having initial aperture efficiency of about 6.8% before encapsulation, showed extensive delamination and a decrease in efficiency to about 0.3% after less than 6 hours of UV irradiation. By comparison, the conversion efficiency for three devices encapsulated with polyester showed insignificant change after 24 hours of high intensity UV irradiation. It appears that the back metal may actually be catalyzing some polymer degradation mechanism for the EVA, but not for the polyester. While it may not be appropriate to interpret these results as important from the standpoint of field application, because the EVA is rarely exposed to high energy irradiation from the rear, these results reveal the comparative robustness of the polyester system.

Based on the encouraging initial results, a recommendation was made to manufacturing to undertake expanded testing of the polyester resin lamination systems, including more advanced accelerated life testing. The potential cost savings and achievable throughput advantages appear attractive.

### **1.7 100 MW Coater Design**

During Phase I the decision was made to proceed with the construction of production equipment utilizing the VTD method for semiconductor film deposition. To fully exploit the high-throughput advantages of VTD for CdS/CdTe, the system design included both the capability for increased web width (to 4 ft) and faster substrate transport speed (to a linespeed of 8 ft/min). Moreover, since glass flow will be continuous, dramatically higher total system capacity will be possible. The system is being called the 100MW coater because if run for three 40hr shifts/week it would produce 1,500,000 CdS/CdTe-coated plates per year (4 modules/min x 60 min/hr x 2080 hr/yr/shift = 500,000 2 ft x 4 ft plates). If these 1,500,000 2ft x 4ft plates/year were finished into 9.3%-efficient modules, the PV production would be 100 MW<sub>p</sub>/year.

Design of the vaporizer and vapor distributors for the large coater involved scaling the high temperature furnace components. The increase from 60-cm-wide to 120-cm-wide webs necessitated a re-assessment of the original design. Long-span furnace components can be fragile and specific attention was given to increasing component strength, improving robustness of connections, and simplifying service and replacement methods. This new equipment will become operational during the second half of Phase II.

## **2. Efficiency Improvement**

Improvement of module conversion efficiency has tremendous leverage in decreasing per watt module costs, decreasing installation and balance-of-system costs, and increasing access to new markets. As a result of these benefits, several projects were pursued with the intent of improving module efficiencies. In addition to the work described below, considerable work described elsewhere in this report was part of the effort to improve efficiencies (for example the diagnostics of section 1.2, the deposition development of section 1.3, the post-deposition development of sections 1.4-1.6, and the characterization of section 3.1).

### **2.1 Small-area experiments**

#### **2.1.1 Thin CdS, buffer layers and TCO treatments**

As was shown in section 1.3.1, the normal CdS thickness that First Solar uses in production is approximately 3000Å. At this thickness, the vast majority of the blue light of the incident spectrum is absorbed in the CdS and these photogenerated carriers are not collected. This presents a key opportunity to increase photocurrent by reducing the CdS layer thickness. However, simply reducing the thickness of the CdS by a large amount with no other changes to the device or deposition processes has been found, in most cases, to decrease cell efficiency due to reduced  $V_{oc}$  and FF. The addition of a high-resistivity layer between the TCO and CdS layers, a so-called buffer layer, has been shown to allow the thinning of the CdS layer (with a corresponding increase in  $J_{sc}$ ) with less loss in  $V_{oc}$  or FF [13-15].

The properties of this buffer layer (or any layer that immediately precedes the CdS deposition) are critical because the layer i) acts as a nucleation aid thus affecting CdS and subsequently the CdTe growth [16], ii) can be harmful to devices if it is unstable in the subsequent processes used [17], iii) can act as a capping layer or a diffusion barrier that minimizes the effect of process instability of prior TCO layers, iv) can modify the electrical behavior of the device in the vicinity of the critical junction [13], and v) can affect CdS adhesion by allowing interdiffusion at the buffer layer-CdS layer interface [14].

##### **2.1.1.1 Zinc stannate buffer layer**

One of the leading candidates for a buffer layer with superior performance is zinc stannate ( $Zn_2SnO_4$ ), recently developed at the National Renewable Energy Laboratory [14]. It has been claimed that the layer improves device efficiency, CdS adhesion, and the reproducibility of device efficiency.

The plan for work on zinc stannate (also called ZTO for zinc tin oxide) at First Solar is to demonstrate a benefit on the small-scale for our devices, develop deposition processes for the layer suitable for high-throughput manufacturing, and then scale the processes to the 60cm x 120cm size. The small-scale device research is progressing on two fronts. The first is a collaborative effort with the inventor of the zinc stannate buffer layer at NREL, Dr. Xuanzhi Wu. Dr. Wu first prepared 4 substrates (3"x3" in size) that consisted of

borosilicate glass, a high-quality chemical-vapor-deposited SnO<sub>2</sub>:F layer, and in two cases, a sputter-deposited and annealed zinc-stannate layer. CdS and CdTe were then deposited at First Solar using the RMS system, which uses close-spaced sublimation. The samples were then given a wet CdCl<sub>2</sub> treatment and the X3 back contact treatments. This first round gave high efficiencies for all of the samples (average of 12.6%) with a champion cell of 13.92% efficiency after 9 days of light soak (810 mV, 23.1 mA/cm<sup>2</sup>, 74.4% FF). While this first round did not show a benefit from the ZTO layer, it clearly demonstrated the increased efficiency that can be achieved with a high-quality substrate.

A second area of device-scale research with ZTO buffer layer was deposition of ZTO at First Solar. The ZTO was deposited on Tec-8 glass (8 Ω/sq SnO<sub>2</sub>:F on soda lime glass from LOF) by RF-sputtering. CdS and CdTe were then deposited using the RMS system; some of the samples were annealed for five minutes at 580°C after the CdS was deposited. All the samples were then wet-CdCl<sub>2</sub> treated and given the X3 back contact treatments. The results showed a broad process space with what appeared to be reduced sensitivity to CdS thickness. Cells as high as 11.4% efficiency were made with unannealed ZTO/400Å-thick-CdS layers.

A third area of effort on ZTO buffer layers is the investigation of alternative methods of deposition for this and other buffer layers. We have begun work with an outside party to investigate atmospheric-pressure chemical-vapor deposition (APCVD) of some of the materials of interest.

#### 2.1.1.2 Sprayed-SnO<sub>2</sub> buffer layer

SnO<sub>2</sub> buffer layers deposited using spray-pyrolysis by Peter Meyers and Scott Albright at ITN were studied as part of the CdTe National Team effort. This buffer layer (it also has been called an HRT layer for high-resistance tin-oxide) was originally developed at Golden Photon, Inc. (GPI) and reportedly helped them achieve 14.7% efficiency on 3mm soda lime glass. The samples for this study were prepared by spray pyrolysis on LOF substrates to a thickness of about 0.8μm. The buffer layers were either undoped or doped with Cd or Zn (doped films are nominally doped at 1%). Of these three HRT layers, Zn doped is the most resistive.

Nine substrates were provided, three from each kind of HRT (undoped, Zn-doped or Cd doped). Devices were made on each different kind of TCO with CdS thicknesses of 0Å, 500Å or 1000Å. The 1000Å was intended to represent a thickness which produces good V<sub>oc</sub> without a buffer layer; 500Å represents a CdS thickness for which V<sub>oc</sub> is expected to be somewhat lower than optimum but will exhibit higher J<sub>sc</sub> than obtained with 1000Å CdS. With an appropriate buffer layer 500Å thick CdS is expected to produce good V<sub>oc</sub> with high J<sub>sc</sub> resulting in an enhancement in performance. The devices without a CdS layer were made to study the quality of the junction between the HRT layers and CdTe.

The CdS (when it was used) and the CdTe layers were deposited by close-spaced sublimation in the RMS system. The films were then given a wet-CdCl<sub>2</sub> treatment and the X1 contacts were applied. The results, which are averages of 8 cells from each substrate, are shown in Table 2.1. The efficiencies after 1 day and 42 days of open circuit light soak (~65C) are shown in Table 2.2

**Table 2.1** Average cell characteristics for substrates with spray-deposited buffer layers.

Buffer layer	Initial efficiency			Initial $V_{oc}$ (mV)			Initial $J_{sc}$ (mA/cm <sup>2</sup> )		
	0Å CdS	500Å CdS	1000Å CdS	0Å CdS	500Å CdS	1000Å CdS	0Å CdS	500Å CdS	1000Å CdS
Undoped	4.9	11.1	11.4	477	726	804	22.7	24.5	20.8
Zn-doped	7.6	11.8	12.0	730	783	815	23.2	22.8	21.5
Cd-doped	6.8	11.1	12.3	601	773	827	23.4	22.8	22.0

**Table 2.2** Average cell characteristics after light soak at open circuit bias for substrates with spray-deposited buffer layers.

Buffer layer	Efficiency at 1day LS			Effic. after 42day LS		
	0Å CdS	500Å CdS	1000Å CdS	0Å CdS	500Å CdS	1000Å CdS
Undoped	9.4	11.6	11.1	5.4	9.0	9.6
Zn-doped	10.9	11.3	11.6	6.2	8.9	9.3
Cd-doped	7.6	11.2	11.8	4.6	8.6	7.5

The following conclusions were drawn from these results:

- Zinc- and cadmium-doped HRT layers seem to marginally improve initial cell efficiency. Although the cells made on undoped HRT had a lower starting efficiency, after continued light soaking the cells with the undoped HRT and a CdS layer had a better efficiency than cells made on doped HRT layers.
- Most of the devices made without a CdS layer were initially poor due to low  $V_{oc}$  and FF. All of the no-CdS cells improved under light soak initially and then rapidly degraded under continued light soak.
- After an initial light soak one of the cells made without the CdS layer had an efficiency of 12.4%, which is probably the highest reported for such a device.
- With decreased CdS layer thickness the  $J_{sc}$  improved, but not as much as would be expected. Researchers at other organizations on the National Team reported an even stronger effect; they got no increase in current with thinner CdS.

### 2.1.2 Improved TCOs

First Solar currently uses Tec-15 substrates from Libby-Owens-Ford (LOF). These substrates consist of soda-lime glass coated with barrier layers plus a doped-SnO<sub>2</sub> layer with a sheet resistivity of approximately 15 Ω/sq. These layers have inferior optical transmission and electrical conduction compared to some laboratory-scale transparent conducting oxides (TCOs). The use of improved TCOs should enable increased efficiency by increasing the photocurrent and decreasing the series resistance. Additionally, alternative TCOs might be less expensive to produce since other requirements that Tec-15 must meet for its main application, low-e architectural glass, can be relaxed.

One of the leading candidates for improved TCOs is cadmium stannate (Cd<sub>2</sub>SnO<sub>4</sub>) [18]. Because in-line deposition of transparent conducting oxides (TCOs) and buffer layers coupled with thin CdS are leading methods of improving efficiency and reducing costs,

we have increased our efforts in this area. We have begun work with an outside party to investigate atmospheric chemical-vapor deposition of some of the materials of interest.

### 2.1.3 Post-deposition treatments

#### 2.1.3.1 Vapor-CdCl<sub>2</sub> treatment

Because non-uniformity in the module can greatly lower FF and V<sub>oc</sub>, we have continued to look to in-line, vapor processes as one way to increase module efficiency. The greater uniformity of the vapor-CdCl<sub>2</sub> treatment process is discussed in section 3.1.2.1. Several experiments were done to map out the vapor-CdCl<sub>2</sub> treatment process space in preparation of scaling the process to module size. Figure 2.1 shows the results of one of those experiments which shows relatively broad process latitude with substrate temperature (from 390 to 460°C) and treatment time (from 5 to 22 minutes).

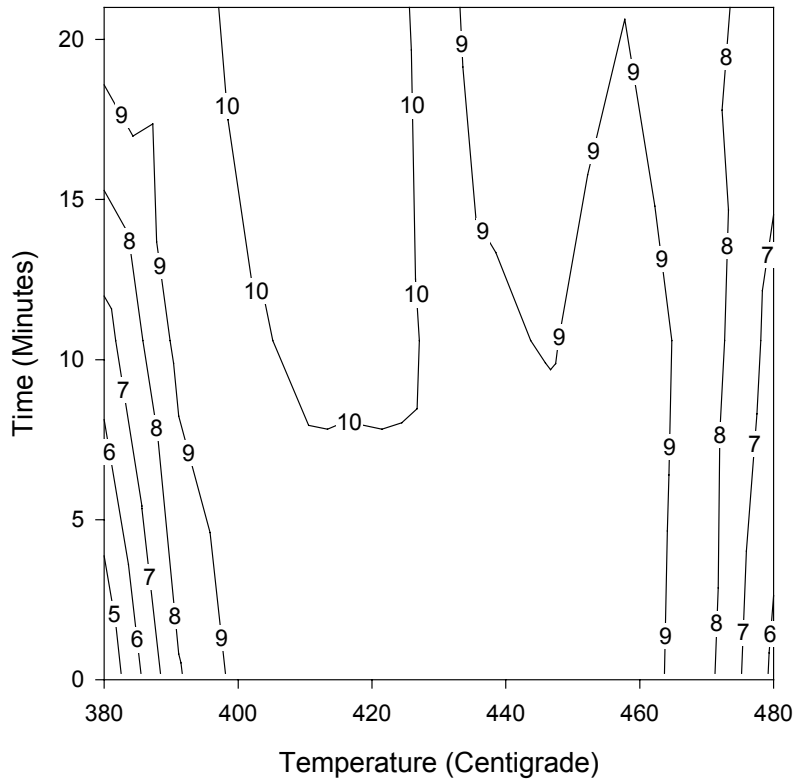


**Figure 2.1** Contour plot of cell efficiencies as a function of two vapor-CdCl<sub>2</sub> treatment variables (substrate temperature and total time).

Additional experiments found the process latitude to be even wider for the source temperature. Variation of the source temperature from 360 to 460°C had very little impact on cell performance. Since the research vapor-CdCl<sub>2</sub> system uses the close-spaced sublimation configuration, the insensitivity to source temperature indicates an insensitivity to the CdCl<sub>2</sub> vapor pressure at the substrate - this result bodes well for scale-up of the vapor-CdCl<sub>2</sub> process.

### 2.1.3.2 Treatment of CdTe with Tellurium Chloride

Although the role of cadmium chloride is not yet fully understood, it is believed that one of the benefits of the treatment is that it can act as a flux that breaks down the atomic diffusion barrier at the grain boundaries thereby promoting grain growth [19]. While other halides have been shown to act as fluxing agents [20], only HCl has been proven to produce benefits comparable to those that CdCl<sub>2</sub> produces. At First Solar, zinc chloride and ammonium chloride have been tried with inconclusive results.

One potential candidate for an alternative flux is TeCl<sub>4</sub>, which would be expected to leave a tellurium-rich layer on the back surface of the CdTe. Te layers have been shown to be favorable for back contacts [21, 22]. Possible drawbacks of using TeCl<sub>4</sub> are its lower melting point (360°C) and poor chemical stability. In aqueous solutions it has the tendency to hydrolyze, forming HCl. For initial experiments, TeCl<sub>4</sub> was applied in the form of aqueous solution similar to the method used for CdCl<sub>2</sub>. Subsequent heat treatments at temperatures higher than 360°C damaged the samples. At about 360°C there was definite evidence of treatment, however, it was not clear whether the treatment was due to TeCl<sub>4</sub> or to HCl produced by the hydrolysis of TeCl<sub>4</sub>.

### 2.1.3.3 Plasma cleaning of vapor-chloride-treated samples

While the vapor-CdCl<sub>2</sub> treatment leaves much less residue than a wet-CdCl<sub>2</sub> treatment, it still leaves some residue which, if not removed prior to contact application, results in high series resistance. Usually a 5-10 second rinse in running DI water is sufficient to remove the residue, which SEM images indicate is CdCl<sub>2</sub> granules condensed on the surface. Replacement of the water rinse with a plasma cleaning would allow for an all-dry back contacting scheme.

Plasma cleaning was tried in a small sputter coater by sticking the sample to a SnO<sub>2</sub> target and back sputtering. Since the target is larger than the sample, it is likely that there was contamination from the target. Four samples were used in the experiment: a control, 20 s sputter, 50 s, and 180 s. The average efficiency of the cells on the sample sputtered for 20 seconds was comparable to the control (9.2% and 9.3% respectively). The efficiency on the samples sputtered for 50 and 180 seconds were 8.8% and 8.5% respectively. This initial experiment indicates that plasma cleaning is an alternative to water rinsing after the vapor-CdCl<sub>2</sub> treatment, but a plasma etching set-up that will not contaminate the sample is needed for further evaluation of the technique. This work will be done under an SBIR contract awarded to First Solar this year.

## **2.2 Large-area experiments**

### **2.2.1 Defect reduction**

Work progressed in understanding the sources of pinholes and reducing their incidence. We believe that some CdTe pinholes are the result of CdS particulate -- source-material-feed experiments done during Phase I contraindicate external homogeneous nucleation as a cause of particulates.

### 2.2.2 Electrical loss reduction

First Solar uses a monolithic integration scheme whereby the films the size of the panel are laser scribed to create and interconnect cells. The first scribe (scribe-1) is made through the entire film stack, including the TCO, to create isolated 1 cm wide cells. The second scribe (scribe-2) is made down to the TCO layer to allow subsequent metal contact from the back metal of each cell to the TCO layer of the adjacent cell. The last scribe (scribe-3) simply cuts the back metal layer to isolate the metal of each cell from the metal of the adjacent cell. In total, there are 116 cells (each 60 cm wide by 1 cm long), connected in series on a 60 x 120 cm module.

Currently, an all-dry contact is being considered as an alternative to the standard First Solar process due to its suitability to high-throughput manufacturing and superior open-circuit stability. The contact, which when placed on wet-CdCl<sub>2</sub> treated CdTe is referred to as the X5 contact and when placed on vapor-CdCl<sub>2</sub> treated CdTe is referred to as the X6 contact, uses a sputtered interfacial layer (IFL) in place of the wet processing currently used. Work was done to evaluate the effect of the contact on laser scribe resistance. Minimodules (10 cm x 10 cm with 9 scribes) and scribe test structures (with 56 scribe-1 and scribe-2) were made -- half with scribe 2 (which allows connection of the back metal to the adjacent cell TCO) done before deposition of the IFL and half with scribe 2 done after deposition of the IFL. For the minimodules, the series resistance of the piece where the scribe 2 was done before IFL deposition was 1.78Ω/scribe while in the other piece it was only .046Ω/scribe. Since a mini module has at least eight scribe-2 lines, if scribe 2 is done before the IFL deposition the additional series resistance due to the IFL contact resistance would be 14.24Ω. The power loss due to this additional series resistance would be close to 30%. The scribe test structure results supported the mini-module result: for the scribe 2 done before the IFL deposition the series resistance was 100Ω (and 86Ω after 1 week of light soak) while the test structure with the scribe 2 done after the IFL deposition had a series resistance of only 2.6Ω (which was unchanged by a week of light soak). These observations show that scribe 2 must be done after the IFL deposition.

### 2.2.3 Modules

Twelve modules were fabricated and shipped to NREL in satisfaction of a Phase I contract requirement. The IV parameters of the modules are shown in Table 2.3. The “alternative encapsulated” module (module ID# K990119-21) on the last row of Table 2.3 was encapsulated using the alternative material system described in section 1.6.

**Table 2.3** IV parameters of modules delivered to NREL.

	Aperture Efficiency	Total-area efficiency	V <sub>oc</sub> (per cell)	J <sub>sc</sub> (mA/cm <sup>2</sup> )	Fill Factor
Average	7.77 %	7.26 %	807 mV	18.7	54.9%
Standard deviation	0.18 %	0.17 %	7 mV	0.3	1.9%
Maximum	8.08 %	7.55 %	815 mV	19.3	56.6%
Minimum	7.49 %	7.00 %	795 mV	18.5	51.2%
Alternative encapsulated	8.04 %	7.51 %	815 mV	18.5	56.6%



## **2.3 Research equipment development**

### **2.3.1 Large-area sputter deposition system**

Given the potential importance of TCOs, buffer layers and alternative back contacts to module efficiency, it was decided to design and build a large-area multi-cathode sputtering system capable of depositing films on 60cm x 120 plates to allow research on the module-size scale. During Phase I, the design of the system was completed and the majority of the parts acquisition and system assembly was completed. The system is shown in Figure 2.2.



**Figure 2.2** Large-area sputter deposition system for research.

One of the key elements of the system design was the magnetron cathodes. After a review of potential suppliers it was determined that AJA International was the best source for the 5" x 30" magnetron cathodes. AJAI units have the magnet array isolated from the cooling water to prevent their degradation and have the targets isolated from cooling water to make target-change easier. One of the advantages of the AJAI magnetron structure is the standard modular magnet array which allows the magnetic field to be tailored to the application; the field can be operated in a balanced configuration or in a variety of unbalanced configurations. In the unbalanced configuration the outer magnets are much stronger than the center magnet, resulting in a magnetic field that extends from the cathode towards the substrate. Electrons spiral along these field lines, ionizing the sputtering gas. The positive ions follow the electrons into the growing film, thus providing low energy ion bombardment. This ion bombardment results in excellent film density and adhesion. In this configuration the sputtering rate is very high. In the balanced configuration both the center and outer magnets are of equal strength resulting in a field that is confined only around the cathode. In this configuration the ion bombardment is minimal; it is useful when very thin and uniform coatings are needed.

The power supply is also an important element in a sputtering system. DC power was selected for this application. While plain DC excitation is suitable for sputtering metals, in the presence of oxygen the discharge can become unstable because of oxide formation on the surface of the target. The plain DC excitation might also pose problems when less conductive targets such as tellurium, or tin oxide are used. To overcome the limitations of the plain DC excitation, the ENI Corporation has introduced a new power supply in which the DC can be pulsed to form an asymmetrical bipolar pulse. As the pulsation is done at a lower frequency, any magnetron designed for DC operation can be excited by this new power supply. The asymmetrical bipolar power supply can also be operated as a conventional DC supply by turning off the pulsation. Since the magnetron power supplies are expensive, in a multi-cathode system it is more economical to use a single power supply to excite all the magnetrons as long as only one is used at a time. For switching the DC power, vacuum relays made by KiloVac Corporation were selected.

### 2.3.2 Small-area vapor-CdCl<sub>2</sub> system

A small vapor-CdCl<sub>2</sub> system, which can treat 10cm x 10cm substrates, was designed and constructed for use as an additional research tool. The system uses a total of twelve 500W quartz heaters inserted into two graphite blocks which control the CdCl<sub>2</sub>-source and the substrate temperatures. The blocks are capable of heating the substrate to 400°C in less than 1 minute; the blocks can also be cooled rapidly by use of a nitrogen gas quench. The rapid thermal response enables testing of all the thermal profiles that would be considered for the production system. The system is computer controlled through a RS-485 computer network that sends commands to the temperature controllers and the air solenoid controller. The system is shown in Figure 2.3.

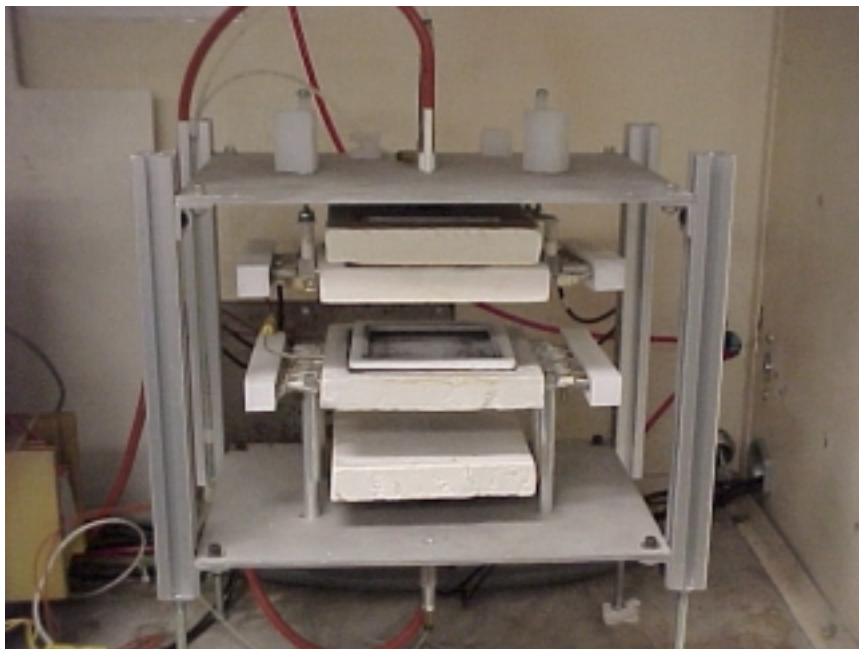


**Figure 2.3** Small-area vapor-CdCl<sub>2</sub> treatment system

### 2.3.3 Small-area VTD system

During Phase I it became clear that many VTD experiments were not practical to conduct using the pilot production system. In addition to access time constraints, some experiments were stifled. For example, experiments involving alternative materials and compositions risk chemical contamination of a system that is producing product for customers. Consequently, an alternative, small-scale VTD system was constructed. This system was built to emulate the larger systems in glass transport and film deposition. However, some differences were inevitable. The small VTD system consists of a mesh belt transport system that moves substrates beneath the deposition injectors. Samples, up to 4" x 8" in size, are introduced through an entrance load lock and are pushed onto the moving belt. The substrates creep through a pre-heat zone and can then be accelerated for transport past the vapor distributors at speeds similar to those used in the full scale equipment. After deposition the substrates slide off the belt into a tray that shuttles into the exit load lock. This system became operational during the fourth quarter of Phase I; it is shown in Figure 2.4.



**Figure 2.4** Research VTD system.

While fine-tuning of the system continues, several new experiments have been conducted. One of the new materials that we are interested in as an IFL candidate is ZnTe. In principle, ZnTe is very similar to CdTe and CdS with a vapor pressure curve intermediate to the two. We began coating ZnTe and defined the process space needed to form well-adherent films. As with CdTe, a minimum substrate temperature and maximum ambient pressure limit were found beyond which homogeneous nucleation occurred. In addition the deposition of ZnTe was very sensitive to oxygen. Not surprisingly, any small leak resulted in rapid ZnO formation. We switched to a reducing gas (4% H<sub>2</sub>) which compensated for small ambient leaks. As grown, the ZnTe films are very resistive. Work has begun on addition of dopants to the growth ambient.

### **3. Characterization and Analysis**

#### **3.1 Characterization of films and devices**

##### **3.1.1 Temperature coefficient**

The temperature-dependence of First Solar modules was studied in order to gain insight into device operation, to better predict total-year output for arrays, and to better interpret field data. The importance of the temperature coefficients for the correct interpretation of field data was reinforced by the measurement of the First Solar array at Edwards AFB (called the China Lake array) -- the use of incorrect temperature coefficients gave a value for array output that was 8% lower than that found using the correct coefficients.

One method used to study the temperature-dependence was IV measurement of modules at two temperatures. Twenty-three modules that had been in the field over a range of times from 3 months to 5 years were measured at room temperature ( $\sim 25^{\circ}\text{C}$ ) and then placed in a temperature booth and raised to  $60^{\circ}\text{C}$ . The modules were then re-measured; due to cooling during transport from the temperature booth to the simulator we estimate the film temperature at time of IV to be  $50$  to  $55^{\circ}\text{C}$ . On average, the efficiency was 2% (relative) higher at  $50^{\circ}\text{C}$  than at  $25^{\circ}\text{C}$  and the  $V_{oc}$  was 6% lower at  $50^{\circ}\text{C}$  compared to  $25^{\circ}\text{C}$ . In the standard notation for temperature dependence, this translates to an average  $P_{max}T$  coefficient of  $0.08\%/^{\circ}\text{C}$  and an average  $V_{oc}T$  coefficient of  $-1.8\text{ mV}/^{\circ}\text{C}$  (the average  $V_{oc}$  at  $25^{\circ}\text{C}$  was  $762\text{mV}$  on a single-cell basis). The standard deviation, however, was 5% on the  $50^{\circ}\text{C}/25^{\circ}\text{C}$  efficiency ratio and 2% on the  $50^{\circ}\text{C}/25^{\circ}\text{C}$   $V_{oc}$  ratio. There was no detectable relationship of the  $P_{max}T$  or  $V_{oc}T$  coefficients with time in the field. It should be noted that earlier tests with more temperature points had indicated a negative  $P_{max}T$  coefficient ( $-0.23\%/^{\circ}\text{C}$  from a mini-module in 1995 and  $-0.34\%/^{\circ}\text{C}$  from a module in 1997).

A second method of study was fitting of field data as a function of temperature. Results are shown in Table 3.1.

Table 3.1.  $P_{max}T$  and  $V_{oc}T$  coefficient calculations from field data ( $V_{oc}T$  for a single cell)

Modules / location	Data-fitting done by	$P_{max}T$ coefficients	$V_{oc}T$ coefficients
4 modules at SWTDI	G. Rich (First Solar)	+0.03%/C	-1.8 mV/C
B14407 at NREL	J. Del Cueto (NREL)	-0.20%/C	-2.2 mV/C
1 kW array at NREL	B. Kroposki (NREL)	-0.15%/C	
China Lake array	D. King (Sandia)	-0.25%/C	-2.9 mV/C

The last entry in Table 3.1 was determined from measurement of array output at two different temperatures with nearly the same irradiance. A large change in ambient temperature on successive days allowed the measurement of array output with module temperatures of  $35^{\circ}\text{C}$  and  $55^{\circ}\text{C}$ . The  $V_{oc}T$  coefficient for the array was  $-2.03\text{V}/^{\circ}\text{C}$  which translates to  $0.338\text{V}/^{\circ}\text{C}$  for a  $90.5\text{V}$  module at  $25^{\circ}\text{C}$  and  $-2.9\text{ mV}/^{\circ}\text{C}$  for  $780\text{mV}$  cells.

### 3.1.2 Contactless measurement of $V_{oc}$

Section 1.2.1.4 described the adaptation of contactless- $V_{oc}$  measurement to the module-scale X-Y table, while this section discusses use of the technique to understand small-area devices. The technique uses a graphite-foam pad and a high-input-impedance voltmeter (an electrometer) to read the “open circuit voltage” of the device before a contact is applied. This technique has also been called SPV, or surface photovoltage, but it differs from classic SPV in that the illumination of the device is from the side opposite the graphite pad; for our technique the illumination is from the “sunny side” of the device at about 0.7 sun intensity.

During Phase I, the contactless- $V_{oc}$  measurement was used to investigate the effect of the  $CdCl_2$  treatment and one type of contact treatment as discussed below.

#### 3.1.2.1 Uniformity after $CdCl_2$ treatment

The average of the contactless- $V_{oc}$  (and standard deviation) of 16 points from an as-deposited 10cm x 10cm piece of glass/ $SnO_2/CdS/CdTe$  was  $598 \pm 2$  mV. A solution- $CdCl_2$  treatment of the material raised the voltage to  $718 \pm 16$  mV. A vapor- $CdCl_2$  treatment of another piece raised the voltage to  $712 \pm 8$  mV. Repeats of the experiment consistently showed that the vapor- $CdCl_2$  treatment yields more uniform voltage than the wet- $CdCl_2$  treatment.

#### 3.1.2.2 Effect of Cu on $V_{oc}$

The contactless- $V_{oc}$  measurement was used to investigate the effect Cu on devices. Cu is one of the options for doping of the CdTe material and preparation of an ohmic back contact. One of the key questions concerning the operation of CdTe solar cells is, “why are treatments at the back contact capable of significantly raising the open circuit voltage of completed devices?” Our studies have indicated the most likely answer is that Cu (or other dopants or effects introduced during the back contact treatments) raises the hole concentration throughout the CdTe layer. Other less likely explanations are that Cu raises the  $V_{oc}$  by altering the grain boundaries or by simply changing the back of the device (e.g., raising the carrier concentration or eliminating fermi-level pinning) which somehow raises the  $V_{oc}$ .

The average of the contactless  $V_{oc}$  (and standard deviation) of 16 points from a wet- $CdCl_2$ -treated 10cm x 10cm piece of glass/ $SnO_2/CdS/CdTe$  was  $718 \pm 16$  mV. After exposure to Cu through a solution process, the  $V_{oc}$  was essentially unchanged. Then, after heat treatment at  $200^\circ C$  for 30 minutes, the  $V_{oc}$  increased to  $822 \pm 12$  mV. From this experiment alone one cannot tell whether the heat treatment was needed to activate an effect of Cu at the back of the device or whether the heat treatment was needed to drive the Cu into the bulk of the CdTe film or into the grain boundaries.

An experiment in which the CdTe was slowly removed from the back of the device by lapping was conducted to try to answer the question of whether Cu was raising  $V_{oc}$  by its presence in the CdTe (in the bulk or in the grain boundaries) or at the back of the device. In this experiment, wet- $CdCl_2$ -treated CdS/CdTe was used; the  $V_{oc}$  before exposure to Cu was 670 mV. After an anneal, thin layers of the CdTe were removed by polishing off the

back surface with 3 $\mu\text{m}$ -grit alumina-coated lapping paper. A 5-second lap with average finger pressure removed about 500 $\text{\AA}$  of material. The film thickness was measured using the Tencor step profiler, which enabled plotting of the contactless  $V_{oc}$  vs. the amount of CdTe removed by lapping. Figure 3.1 shows the contactless  $V_{oc}$  for three cases as a function of CdTe removed by lapping: a) Solution exposure to Cu and 30min 200 $^{\circ}\text{C}$  anneal, b) case “a” re-exposed to Cu by the same process and re-annealed after 5000 $\text{\AA}$  CdTe had been removed by lapping, and c) 10 $\text{\AA}$  sputtered Cu with 30min 200 $^{\circ}\text{C}$  anneal.

Figure 3.1, curve “a” indicates that the effect of Cu on  $V_{oc}$  was eliminated after removal of about 3000 $\text{\AA}$  of material. Figure 3.1, curve “b” indicates that re-exposure and re-anneal of the sample yields similar behavior to the “a” case. Curve “c” indicates that the behavior of the sample to 10 $\text{\AA}$  of sputtered Cu is similar to that of the company-confidential Cu application process.

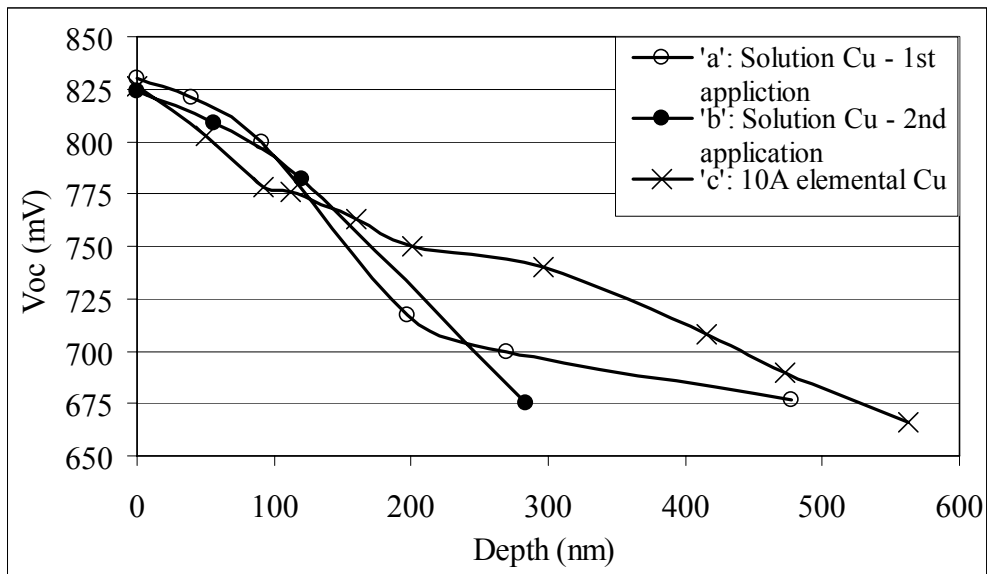


**Figure 3.1** Contactless- $V_{oc}$  as a function of CdTe material removed by lapping.

While it would seem that the above experiment proves that Cu somehow raises the  $V_{oc}$  of the device by some action only at the back of the device, there are alternative interpretations. The lapping of the CdTe could be introducing defects in the CdTe layer that affect the CdS/CdTe junction quality. A commonly cited rule of thumb is that lapping will damage a film to the depth of the grit diameter. Thus, 3  $\mu\text{m}$  grit lapping paper would be expected to damage the 3 $\mu\text{m}$ -thick film to the junction. The re-exposure to Cu and 2<sup>nd</sup> heat treatment could have annealed these lapping-induced defects. Still another interpretation is that the contactless- $V_{oc}$  measurement can be influenced by band bending at the free-CdTe surface. Damage of the surface by lapping could influence this band bending. Additional experiments will be performed to answer the question of whether the Cu is primarily raising  $V_{oc}$  by some action at the back of the cell or through action deeper in the CdTe layer. The mechanism for Cu doping of CdTe is discussed in the next section.

### 3.1.3 Photoluminescence studies

Photoluminescence (PL) has very good sensitivity to the electronic states of impurities in semiconductors, although interpretation of the spectra is relatively complex. We applied PL to the study of Cu-related states in CdTe with the goal of understanding the role of Cu in CdS/CdTe solar-cell devices. In particular, we would like to examine the very good p-doping properties of Cu and its possible role in device degradation. We suggest that Cu introduces two type of acceptor states: a substitutional state and a state related to the formation of  $\text{Cu}_i\text{-V}_{\text{Cd}}$  Frenkel type complexes. These states have a metastable behavior: they are removed/dissociated in time; a re-anneal partly restores these acceptor states. Some of the results have been also discussed in [23, 24]; a detailed discussion is given in [25].

Figure 3.2 illustrates the changes in the PL spectra of *single crystal* CdTe following diffusion (1 hr. 200°C) with Cu from an elemental layer deposited on the surface. Following diffusion, the excess Cu and Cu oxides are removed from the surface of the CdTe by a 10 min etch in 0.01% Br:MeOH.

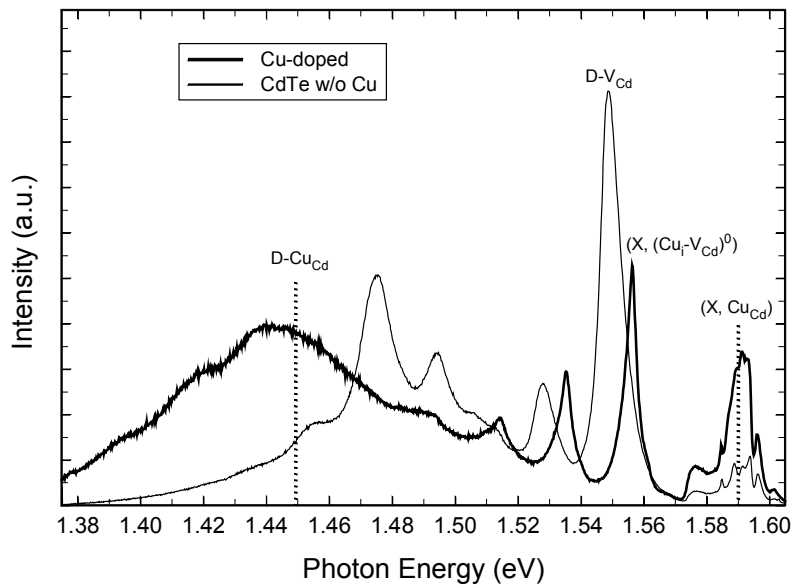


**Figure 3.2** Effects of Cu doping on the PL spectrum in single crystal CdTe. PL excited with 752.5nm radiation of a Kr laser, taken at 10K.

It can be noticed that after diffusion with Cu, a strong line at about 1.59eV (X,  $\text{Cu}_{\text{Cd}}$ ) dominates the excitonic region of the spectrum, while a new donor-acceptor pair (DAP) transition emerges at about 1.45eV ( $\text{D-V}_{\text{Cd}}$ ). At the same time, a DAP transition at about 1.55eV is quenched. These effects are consistent with Cu occupying substitutional positions on the Cd sub-lattice, denoted by  $\text{Cu}_{\text{Cd}}$ . According to previous results and consistent with our data, this creates an acceptor state with an ionization energy of



approximately 150meV. Note that the ionization energy for the Cd vacancy ( $V_{Cd}$ ) acceptor is about 50meV.

In time, both the  $Cu_{Cd}$  and the  $Cu_i-V_{Cd}$  states are removed/dissociate as seen in Figure 3.3. A significant drop in the overall luminescence efficiency is observed for the “aged” sample consistent with the formation of non-radiative recombination centers. It is possible that these centers are related to the formation of Cu precipitates. A re-anneal (1 hour, 200°C) partly restores the PL spectrum indicating that the Cu acceptor states are recovered in part. The drop/recovery of the Cu acceptor states are supported by results of Hall measurements on polycrystalline samples as well as from observations of open-circuit voltage for devices doped with Cu.

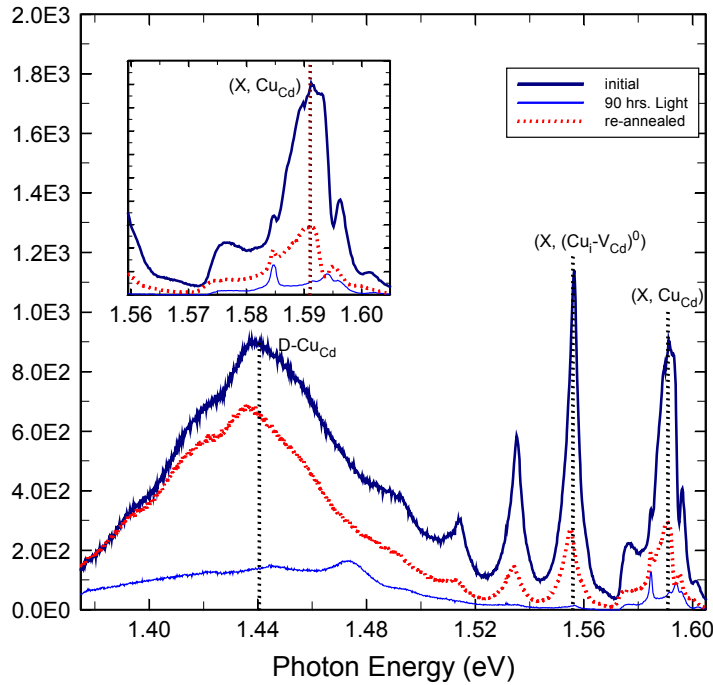


**Figure 3.3** “Aging” effects of Cu-doped CdTe single crystal sample.

In summary, Cu introduces acceptor states in CdTe and as such it could lead to the improvement seen in the open-circuit voltage of CdS/CdTe devices fabricated with Cu. However, Cu states can be unstable leading to a drop in the acceptor concentration from the original value as well as to the formation of non-radiative recombination centers. In turn, these effects could lead to a reduction in efficiency due to lower open-circuit voltages, short-circuit currents, and fill-factors. The implications of these results are discussed in section 3.2.3.2.



### **3.1.4 X-ray diffraction**

The X-ray analysis of selected substrates from the study of wet CdCl<sub>2</sub> treatment of CdTe as a function of time and temperature revealed information on the preferred crystallographic orientation of CdTe. The orientation of the as-deposited samples was mainly <111>. After various CdCl<sub>2</sub> treatments, the orientation rearranged, augmenting the degree of the <220>, <311>, <400> and <331> orientations. The rearrangement of the orientation appeared to be proportional to the extent of the CdCl<sub>2</sub> treatment received.

### **3.1.5 IV(T)**

Measurements of IV(T), both light and dark IV as a function of temperature, were done on small-area devices. This technique can be used to estimate the energy of a back barrier that leads to “roll-over”. The system used for the measurement is capable of sweeping the voltage higher than in other available IV systems and extends the data past the roll-over into another ‘turn-on’ region. The high voltage turn-on may be break-down of the back-barrier but it has a curious temperature dependence and occurs at high enough voltage that a re-examination of the current transport in this region is warranted. The characterization of the extended range IV(T) sweeps could provide clues about the mechanisms of operation of PV devices. For example, even fresh devices with good IVs at room temperature exhibit ‘roll-over’ when cooled significantly. Moreover, devices with interfacial layers (IFL) having the X1 proprietary formulation exhibit IV(T) curve families similar to those of the standard recipe. A review of existing analysis approaches indicated that separating out the effects of voltage-dependent photocurrent should allow for simplified modeling of a barrier at the back contact. Closed-form analysis of this type and computer modeling with the AMPS program is planned.

## **3.2 Reliability Verification and Improvement**

### **3.2.1 Accelerated-test, measurement and tracking systems development**

#### **3.2.1.1 Light-soak equipment development**

A new 4.5ft x 17.5ft station for room-temperature-ambient light soak of cells and modules was installed at the First Solar Research Center. The system uses 28 metal halide lamps in reflectors situated 33” above the samples. The lamps are Lithonia THP-1000M-A22U and the bulbs are GE MVR1000/U (available from Grainger as part #2V659). The light intensity at the sample plane was measured to be 730 W/m<sup>2</sup>, with a standard deviation of 110 W/m<sup>2</sup>. Fans are used to keep a constant air flow under and over the samples. Sample temperature does vary with ambient temperature, but is typically between 58 and 66°C.

The existing light soak station at the First Solar facility on N. Westwood Ave., which uses a configuration similar to that of the Research Center, was also expanded. It now is capable of light soak of up to eight 60cm x 120cm modules at once.

Progress was also made on environmentally-controlled light soak stations: the design and initial mock-up was completed. The stations will be built at the First Solar Research

Center and will allow for temperature control between 50° and 100°C as well as ambient-gas control (air or nitrogen). Each station will allow the light soak of twelve 10cm x 10cm samples under controlled conditions.

#### 3.2.1.2 Datalogging for Toledo arrays

The datalogging system for the TECO array was repaired and upgraded. The TECO array, which is described in more detail in section 3.2.2.1, is located in Toledo, OH and will consist of 10 rows of modules, for a total nominal power output of 100 kW. The first row was completed in July 1995. In the fall of 1997 lightning damaged the TECO data acquisition system which caused a disruption in data accumulation. Repair of the system required the installation of signal conditioners and a data logging system. All of the needed parts were purchased and the components for the monitoring system were built. The data logger was sized to handle the whole field of 10 rows. The monitoring system has been completed, tested and placed into operation.

#### 3.2.1.3 Simulator improvements

The operating system of the computer that operates the module simulator was upgraded to Windows95 and the data-acquisition drivers were updated. A database was implemented for the simulator that allows the storage of recipe codes for all processes, greatly enhancing our ability to track and sort experiments. The codes have been synchronized with the SOP structure currently in operation.

Programs were also created and/or updated for the plotting of IV information. One program, DBplot32, works in conjunction with the Access database implementation Datahub. A macro allows one to shell to the plotting program, Dbplot2, and create many different types of graphs and histograms. Another program, called 'Overlay', which allows users to put multiple IV curves on a single graph, was upgraded to Visual Basic 5 and 32 bit format.

### **3.2.2 Documentation of reliability of devices, modules, and arrays**

This section contains data on the stability and reliability of devices, modules, and arrays. Reliability refers to package integrity and stability refers to constancy of power output over time when there is no loss of package integrity. First Solar modules have been showing good reliability and the lamination changes described in section 1 of this report should improve that performance further. Stability is a more complex issue with many satisfactory results and some that show need for improvement and increased understanding. It should be noted that in both outdoor data and light-soak tests there are examples of cells and modules that have received *very* long term exposure with no degradation at all; thus, it is clear that degradation processes in our devices can be avoided -- one of our key objectives is to determine the degradation modes and mechanisms so that we can insure that the stability will be excellent every time.

#### 3.2.2.1 Outdoor data

The most reliable data for performance of First Solar modules in the field is the 1kW array at the National Renewable Energy Laboratory (NREL). This array, which consists of 24 modules, was installed in June of 1995. Figure 3.4 shows the DC power output for

the array for the four years it has been in the field. Ben Kroposki of NREL performed additional analysis of the data; he averaged the normalized power output for the array and found it to be approximately 1080W in July of 1995 and 1071W in July of 1998, a drop of only 1%. Despite the overall excellent performance, Figure 3.4 may be indicating a small drop in the performance in the most recent year in the field. Analysis of IVs that Mr. Kroposki took on two days of similar irradiance and module temperature in 1996 and 1999 (4/15/96 and 3/3/99) shows that if there is any degradation, it is not in the open circuit voltage. From the IVs of those 2 days, the  $V_{oc}$  of the array was 2.2% higher in 1999 than in 1996. The  $I_{sc}$  and FF were both about 3.3% lower which may indicate a cleaning or measurement problem, increased array mismatch, or increased module series resistance.

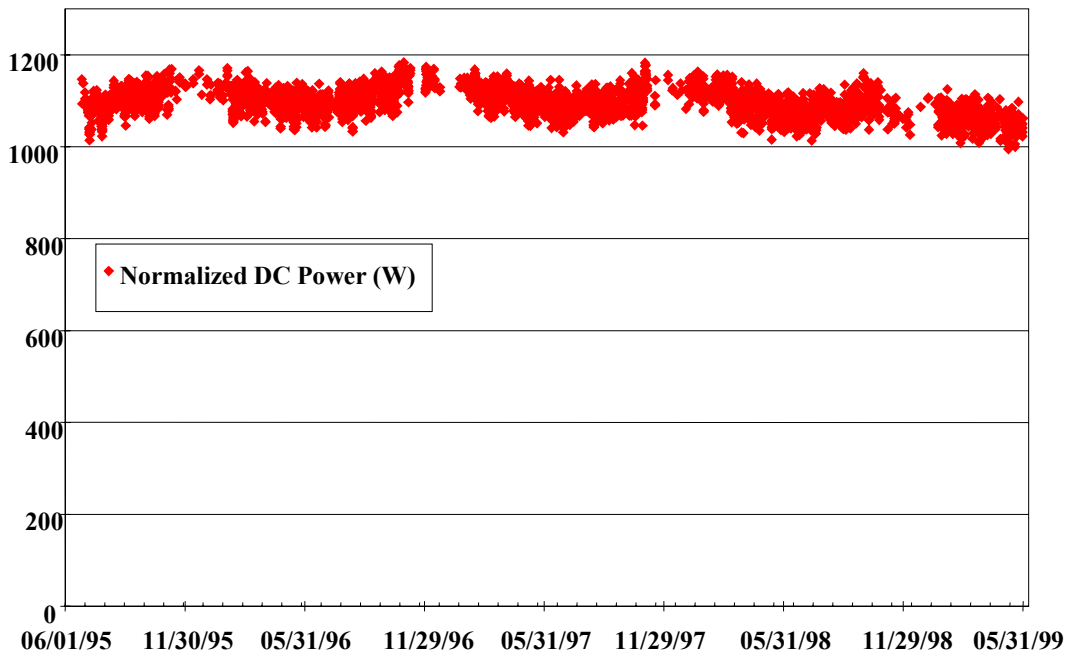


**Figure 3.4** DC Power (normalized to 1000  $W/m^2$  and not temperature corrected) of 1kW-nominal First Solar array at NREL in Golden, CO.

PVUSA array

The First Solar array at PVUSA (Photovoltaic Utility-Scale Array program; installed in October of 1995 as a Solar Cells, Inc. array) has also been performing very well. The 1997 PVUSA report was received during Phase I and it gave the array the highest performance index of any of the PVUSA systems. The First Solar array received a rating of 97 which was higher than for any other Emerging Technology system (which ranged from 4 to 83 and averaged 44) and any Utility Scale system (which ranged from 19 to 86 and averaged 61 not counting the three systems with an index of 0). Reaction to the great rating should, however, be tempered with the realization that the performance index is primarily a rating of the system reliability over time and is thus affected more by inverter uptime and module integrity than subtle changes in power output.

### China Lake array

The First Solar array at Edwards Air Force Base in California (normally referred to as the “China Lake array” since the contracting agency was the Naval Weapons Center at China Lake) also provided some encouraging results during Phase I. The array, which consists of 624 modules and is nominally 25kW, was installed in February 1996. The performance of the array was of particular interest because:

- 1) the majority of the array consisted of modules that were similar in construction to modules and cells that degraded under accelerated testing if they were stressed in the open circuit condition, and
- 2) the array was kept almost exclusively at open circuit for three years in a hot climate. Based on accelerated tests on modules (which seemed to be supported by accelerated tests on cells), Tom McMahon of NREL had predicted that the array would have degraded by about 14% between the 5/97 and 11/98 measurement dates and possibly 25% since installation.

Dave King of Sandia, with support from two of his technicians and Geoff Rich of First Solar, measured the output of the array on 11/18/98. The only previous measurement of the array was by Dave King on 5/20/97. For 25°C with 1000 W/m<sup>2</sup> AM1.5 illumination, the following array power outputs were estimated:

- Power at 2/96 installation\*: 27.1 - 28.6 kW
- D. King’s 5/20/97 measurement: 27.7 kW
- D. King’s 11/18/98 measurement: 26.9 kW

These estimates would indicate a change in the range of +2 to -3% in the first year in the field and then a degradation of approximately 3% in the following two years. There is a high degree of confidence in the estimate of change between the 5/97 and the 11/98 measurements because there were measurements taken on both dates with similar irradiance and temperature. \*Note: The starting power for the array is only an estimate - the array was not measured at time of installation; using production records and assuming the line/mismatch loss is between 5 and 10% provides an initial power range of 27.1 - 28.6 kW for the array.

The better-than-predicted performance of this array is encouraging in terms of product quality, but it does raise questions about our current life-prediction capability. The disagreement between the predictions and the field performance could indicate that the accelerated tests/models currently available to the CdTe National Team are not yet capable of accurately predicting field performance; alternatively, the modules in the array could have been more stable than the modules and cells used for the accelerated-life tests.

### Modules at SWTDI

First Solar has 4 modules in outdoor test at the Southwest Technology Development Institute (SWTDI) in Las Cruces, NM. The modules, which were installed in February of 1995, are individually kept at maximum power point except when the IVs are automatically taken once per hour. Operating temperature histograms as well as performance data have been assembled. After four years in the field the modules are showing approximately 2% power loss per year. This loss, which is higher than that seen for the NREL or PVUSA arrays described above, could be the result of the higher

temperatures of the site, an artifact of the IV sweep process, or some module instability (from cells or a module-component such as bus-bars) that is inconsistent in magnitude.

#### Toledo Arrays

First Solar has three arrays in Toledo, OH; they are referred to as Array 1, Array 2, and the TECO array. Array 1 was installed in early 1993 and has been supplying power to a resistive load. The modules in this array, however, were found to be unstable and several key process steps (such as back contact metal, bus-bar material, and encapsulation procedures) were changed to eliminate the problem in future products.

Array 2 is comprised of modules made in the summer of 1994. The array has a nominal output of 1.2kW and has been supplying power to the grid since its installation. Data tracking of the array output may be indicating a loss of 2%/year, but some of this may be from increased mismatch in the array. Four modules were brought in from the array. On average the efficiency was down only 3% (0.6%/year), but one module was 7% lower than when fielded and one was 7% higher.

The TECO, or Toledo Edison Co. array, is located on the campus of the University of Toledo, in Toledo, Ohio. The array, when completed, will consist of 10 rows of modules, for a total nominal power output of 100 kW. The first row, in excess of 10 kW, was completed in July 1995. In 1998 the construction of the array resumed and is now over 30% complete. The array has modules with various manufacturing details and is comprised in part of modules that were below specification for other projects. The output of Row 1 of the array has been periodically measured, but there are only a few data points per year; fitting of this data may indicate a degradation rate of 2.7%/year. Most modules in rows 2 and 3 have been kept in the short circuit condition since installation. Modules brought in from the array that were fielded between 1994 and 1995 and kept in the short circuit condition have degraded by 0.5%/year. Modules brought in from the array that were fielded between 1994 and 1995 and kept in the loaded condition had actually *increased* in efficiency by 1%/year.

#### Modules at FSEC

First Solar had 11 modules in outdoor test at the Florida Solar Energy Center (FSEC) in Cocoa, FL. The modules were made in April-May 1996 and installed in September 1997 with a maximum power-point tracker (MPT). Because of repeated failures of the MPT, the MPT was replaced by a fixed resistive load. FSEC issued a report (FSEC-CR-1049-98) which included a plot of the normalized array output from September 1997 to November 1998 which appeared to indicate a drop from approximately 500 W to 420 W. The initial drop in the first summer was attributed to increasing mismatch between the array and the fixed resistive load and a step drop of 11% in March 1998 was attributed to wiring changes and checks done over the course of a month. Since it could not be determined from the array output data if the individual modules had degraded, three modules were returned to First Solar. The three modules were measured on the same simulator used when they were fabricated; it was found that the average loss was 5% relative to the IVs taken after the hi-pot tests and 6% relative to the final IVs taken before shipment to FSEC (which was taken after light soaking the modules an average of 16 hours).

### 3.2.2.2 Accelerated life tests

The IV measurements for the first round of stability tests for the CdTe National Team were completed. The cells were re-measured (at 9700 hours of light soak) just prior to the team meeting in September 1998. Mini-modules from the set were also measured at 9700 hours light soak and removed from test. The results (for cells and mini-modules made at First Solar and for cells made by other team members on First Solar CdTe) were presented at the Team meeting and were included in the minutes of the meeting.

Analysis of the results for the mini-modules indicated that of this set the most stable long-term mini-modules were made with vapor CdCl<sub>2</sub> and traces of copper in the IFL layer (they also happened to be un-encapsulated). Analysis of the cell sets revealed no dramatic new information, with recipe X5 (wet CdCl<sub>2</sub>, plus IFL) being the best in the lot. For recipe X5, light soak tests at 100°C required at least 10,000 hrs of test for significant loss to occur. A plot of the normalized efficiency for light soak at 100°C for the X5 cells is shown in Figure 3.5. Also during this time, experiments with small devices indicate that the X6 recipe (vapor CdCl<sub>2</sub> combined with IFL) may be even better than each improvement alone.

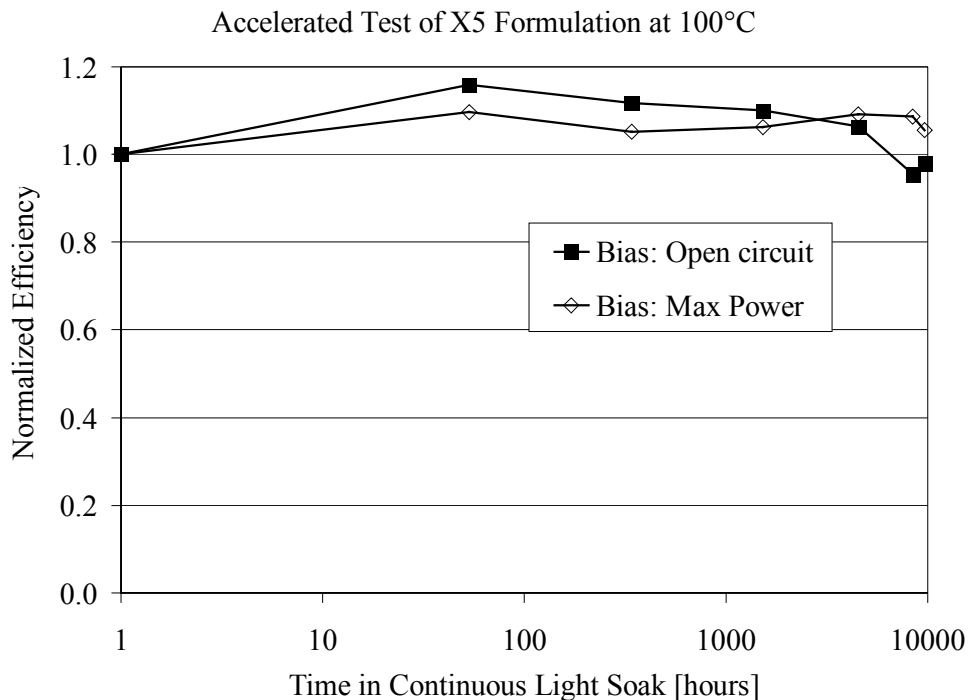


**Figure 3.5** Accelerated test of “X5” cells (wet CdCl<sub>2</sub>, plus IFL).

Accelerated life tests were also done on the cells made for the buffer layer experiments discussed in section 2.1.1. The results of the experiment on substrates provided by NREL (with borosilicate glass, CVD SnO<sub>2</sub>, and in some cases a sputtered zinc stannate layer) are shown in Table 3.2. The semiconductor layers for these cells were deposited with the small-area CSS system (the RMS system) which has been found to be more susceptible to degradation in open-circuit light soak. The results shown in the table may indicate increased open-circuit-stress stability from the ZTO layers.

**Table 3.2** Average cell IV characteristics for substrates with and without a zinc stannate buffer layer, initially and after 68 days of open circuit light soak at ~65°C.

Sample #	Buffer layer	CdS thickness	Initial Effic. (%)	Eff @ 68 days	Initial V <sub>oc</sub> (mV)	V <sub>oc</sub> @ 68 days
NREL-S1-1	ZTO	600Å	12.2	11.4	782	780
NREL-S1-2	ZTO	600Å*	12.6	10.7	805	764
NREL-S1-5	none	600Å	13.0	10.5	807	739
NREL-S1-6	none	1100Å	12.8	9.6	814	720

\*Note: Sample NREL-S1-2 was inadvertently taken out of the deposition system after the CdS deposition, then put back in for the CdTe deposition.

And finally, since for most contact formulation the cells show little or no degradation from light soak when a resistive load is used to place the cell near the maximum power point, we frequently use the open circuit light soak (which causes severe degradation in some cases) to investigate stability. Tracking of the behavior of these open-circuit light soak tests has revealed that material (substrate through CdTe) that has been produced in the past 1.5 years on the large production machine is more susceptible to producing cells that are less stable in open circuit light soak than previous material. Tests are in progress to verify this observation, to identify the variables involved, and to determine if the difference in behavior is affecting the stability of encapsulated modules. Initial tests with encapsulated modules have been encouraging; however, given the importance of excellent stability, additional work will continue with a high priority.

### 3.2.3 Failure-mechanism research and mitigation

#### 3.2.3.1 Process variable identification

Several experiments have been done to identify the process variables that affect cell stability in accelerated life testing (ALT). These experiments indicate that the process variables associated with the back contact are the primary determinants of this ALT stability for our devices. The contention that back contact variables are the primary variables is supported by the observation that cells made using the contact procedures of some of the other National CdTe Team members on our material can be far less stable in accelerated testing than any of our in-house contact options.

In addition to verifying back contact variables as primary, the experiments also identified some potential secondary variables to ALT stability. One of those variables is the substrate used. The results of Table 2.2 (section 2.1.1.2) showed that substrates with a Cd-doped SnO<sub>2</sub> buffer layers produced cells that were less stable than substrates with other buffer layers or no buffer layers. Table 3.2 appears to indicate superior stability of devices with a ZTO buffer layer. Another experiment indicated better-than-typical stability for substrates with a sputtered i-SnO<sub>2</sub> buffer layer and substrates produced by an alternative glass/TCO vendor. Other experiments, however, showed that small variations in substrates or cleaning procedures did not affect the ALT stability.

Additional experiment showed that the substrate temperature during CdS and CdTe deposition did not have a consistent effect on the ALT stability. For depositions in the

small-area CSS system, increasing substrate temperature in the range of 500 to 615°C marginally improved ALT stability, while in the small-area vapor transport system the opposite trend was observed.

Finally, process parameters of the CdCl<sub>2</sub> treatment were investigated. Temperature and process time were found to affect ALT stability, but not in a large or easy-to-understand manner. Most surprisingly, the amount of water in the CdCl<sub>2</sub>-in-methanol solution was not found to affect stability. This variable was investigated since it has been reported that water in the CdCl<sub>2</sub> is detrimental to efficiency [26]. Instead, we found that an aqueous CdCl<sub>2</sub> solution was capable of producing cells with over 11% efficiency that had excellent stability in accelerated tests. Additional work is in progress.

### 3.2.3.2 Contact research

Since contact formulation has been identified as the most important variable in First Solar cell stability and alteration of contact formulation could potentially raise module efficiency and lower production costs, alternative contacts were investigated. However, since the standard First Solar contact has been shown to be capable of excellent stability and has been demonstrated to have wide process latitude that is suitable for high-throughput manufacturing, any alternative must perform quite well to be considered a viable option.

The near-term alternative to the standard contact is the all-dry process, sputtered IFL contact briefly described in section 2.2.2. This contact is more suited to high-volume manufacturing and has repeatedly shown to be more stable in open-circuit light soaking than the standard contact which uses wet processing. The difference is most remarkable for cells made on material that is vulnerable to degradation. Table 3.3 shows data for mini-modules that were light soaked at open circuit and with a resistive load (at ~65°C) for 120 days. The efficiency of the dry-contact mini-modules is lower than typical due to higher series resistance of the scribes of this set.

**Table 3.3** IV parameters for 10cm x 10cm mini-modules with standard contacts and all dry contacts as a function of days light soak (on material that demonstrates vulnerability to ALT instability).

	Open-circuit light soak (~65°C)				R-load light soak (~65°C)-----			
	Wet contact		Dry contact		Wet contact		Dry contact	
Light soak time (days)	Eff (%)	V <sub>oc</sub> (mV)	Eff (%)	V <sub>oc</sub> (mV)	Eff (%)	V <sub>oc</sub> (mV)	Eff (%)	V <sub>oc</sub> (mV)
0	9.9	831	7.8	783	9.8	834	7.9	783
1	9.5	785	8.0	752	10.6	819	7.7	746
7	8.0	751	8.3	759	10.3	815	7.7	743
14	7.6	739	8.4	764	9.9	815	7.8	746
28	7.3	728	8.3	767	9.8	811	7.6	748
42	7.2	719	8.3	762	9.5	809	7.7	746
57	7.0	711	8.3	762	9.4	807	7.6	744
82	7.0	700	8.2	750	9.6	804	7.6	728
120	6.8	695	8.2	756	8.9	792	7.6	732



Another alternative contact investigated was a Cu-free contact using antimony telluride ( $\text{Sb}_2\text{Te}_3$ ). A research group in Italy has been able to fabricate cells with 15% efficiency using sputtered  $\text{Sb}_2\text{Te}_3$  as an IFL [27]; they claim the cells are very stable because no Cu is used. Two parallel efforts were pursued to evaluate the suitability of the process to our devices. The first was to send glass/ $\text{SnO}_2$ / $\text{CdS}$ / $\text{CdTe}$  substrates to the Italian group for contacting. The results were mixed. The cells showed no visible degradation after exposure to 20 sun-illumination, the FF were all above 66%, and the  $J_{sc}$  appeared normal (the exact  $J_{sc}$  could not be measured due to uncertainty of cell area). The maximum  $V_{oc}$  achieved, however, was only 760mV with the average around 700mV.

The second effort with  $\text{Sb}_2\text{Te}_3$  was to investigate the sputtering of  $\text{Sb}_2\text{Te}_3$  layers and the resultant material parameters. The group in Italy sputters at 300°C to a thickness of 2000Å with a resultant resistivity of about  $10^{-4}\Omega\text{cm}$ . Since we do not have the facility to heat the film during sputtering, we deposited the film at room temperature and then heat-treated the film at 200 and 300°C for 30 minutes. The deposition rate at 200W was 1000Å/min. The resistivity was  $0.56\Omega\text{cm}$  as-deposited,  $2.6 \times 10^{-2}\Omega\text{cm}$  after the 200°C anneal, and  $2.05 \times 10^{-2}\Omega\text{cm}$  after the 300°C anneal. The relatively low resistivities of these layers is encouraging and work will be continued.

### 3.2.3.3 SIMS analysis

A detailed analysis was completed of Secondary-Ion Mass Spectroscopy (SIMS) profiles taken on First Solar material by Sally Asher and Matt Young of NREL. X1- and X3-contacted cells that had been light-soaked at 100°C for 4500 hours under reverse bias, load, and open circuit were compared to cells that had not been stressed. Converting the profiles into a tabular format revealed that Cu and Na changed somewhat systematically with stress condition, while Al, Cd, Cr, Fe, Ni, S, Te, C, Cl, O, and Si did not. Table 3.4 gives the Na and Cu levels in the stressed cells as a ratio to the Na and Cu levels in the unstressed cells. It can be seen from the table that changes in Cu concentration are not sufficient to explain the difference in stability of X1 and X3 contacts (the worse bias condition for X1-contacted cells is reverse bias, while open circuit is worse for X3 cells). In fact, there was a better correlation between loss of Na and loss of efficiency than there was with increase in Cu and loss of efficiency. This contraindicates the theory that diffusion of Cu to the junction is the primary degradation mechanism for  $\text{CdS}/\text{CdTe}$  cells.

**Table 3.4** Na and Cu levels in stressed cells (using slow sputtering SIMS result for value in CdS and fast-sputtering SIMS result for value in CdTe)

Cell-bias during light soak:	SIMS ratio in stressed cell to control cell:						Cell performance:		
	In CdS layer		In CdTe layer		Average (CdS&CdTe)		Change at 4500 hours:		$R_{oc}$ at 4500 hours
	Na	Cu	Na	Cu	Na	Cu	in Effic.	in $V_{oc}$	
X1-Rev	0.5	2.2	0.5	0.9	<b>0.5</b>	1.5	<b>-71%</b>	-30%	45
X1-Load	0.9	11.7	2.2	1.3	1.6	6.5	+11%	+1%	6
X1-OC	0.9	18.9	1.7	3.7	1.3	<b>11.3</b>	<b>+10%</b>	+4%	7
X3-Rev	1.4	0.4	1.4	1.0	1.4	<b>0.7</b>	<b>-51%</b>	-23%	45
X3-Load	0.7	5.3	0.7	4.3	0.7	4.8	-27%	-2%	43
X3-OC	0.3	3.9	0.2	0.7	<b>0.2</b>	2.3	<b>-74%</b>	-13%	755

Since the samples used for the SIMS analysis were lifted off of the substrate and then analyzed from the “CdS” side, we had good data on impurity concentration near the CdS/CdTe interface and in the CdTe, but poor data on the back of the sample. Future analysis will focus more on changes at the back contact and will be part of the effort to understand how the back contact can influence  $V_{oc}$ . It should be noted, however, that SIMS only provides information on the overall concentration of Cu, not its bonding state or whether it is in the CdTe lattice or is segregated at grain boundaries.

#### 3.2.3.4 Cu-complex research

Instabilities associated Cu have been identified by the CdTe National Team as important to understanding changes in performance of most CdTe solar cells with stress. As part of that effort we have carried out both parametric studies with cells, which were described in section 3.2.2.2 and 3.2.3.1, and fundamental studies of Cu-complexes using photoluminescence, which were described in section 3.1.3.

#### 3.2.3.5 Cell modeling

From experiments done by First Solar and other members of the CdTe National Team we have observed that a variety of preparations for the back contact (for instance, a Cu diffusion) increase the  $V_{oc}$  of the cell. We have also observed that a decrease in the  $V_{oc}$  can be one of the primary degradation modes in accelerated testing. We thus believe that focusing on the question of “how can the back contact raise  $V_{oc}$ ?” will allow us to improve both the efficiency and stability of CdS/CdTe devices.

Modeling was done to determine the effect of a blocking diode at the back contact. The modeling was done with the following assumptions: 1) the diodes are discrete (no photogenerated minority carriers make it to the back diode by drift or diffusion; the back diode does not influence the energy bands in the active region of the device), and 2) the back diode has no photocurrent. The results showed that while a non-illuminated “discrete” blocking diode can greatly reduce the FF of a device, it cannot influence the  $V_{oc}$ . Since the back contact greatly influences  $V_{oc}$ , a more complicated model is required to explain the first-order behavior of cells.

Modeling was also done in SimWindows and AMPS to try to understand how the back contact can influence  $V_{oc}$ . Both programs indicated that for an acceptor concentration of  $1e15 \text{ cm}^{-3}$  in the CdTe, there is only a very small increase of  $V_{oc}$  with the addition of a higher-doped layer at the back. If the bulk concentration is significantly less than  $1e15 \text{ cm}^{-3}$ , then a higher-doped layer at the back is helpful, but the cells are still very poor since the electric field in a 4- $\mu\text{m}$ -thick n-i-p structure is very low.

## **4. Environmental, Health, and Safety**

### **4.1 General program**

#### **4.1.1 Emissions survey**

A comprehensive emissions survey of the First Solar pilot-production facility was conducted in February 1999. The survey predicted that the air emissions for cadmium would be 0.0015 lb/day for 360 modules/day production using the present process, well below the regulated limit of 10 lb/day. This entitles First Solar to a “De Minimis” Source Exemption for Cd emissions. Process improvements described elsewhere (sections 1 and 4.2 of this report) have reduced the emissions levels even further from those estimated in the February 1999 emissions survey.

The survey did indicate potentially higher than “De Minimis” levels of volatile organic compound emissions, but with the subsequent elimination of the isopropanol rinse, the air emissions for volatile organic compounds for the current process of 20 modules per day is under the regulated 10 lb/day limit. Increase to 360 modules per day will necessitate air permitting if process changes currently under consideration are not implemented.

The details of the emissions survey are given in the Appendix.

#### **4.1.2 Health monitoring**

Cadmium medical monitoring of First Solar employees is scheduled at every year for scientists, technicians, and maintenance personnel, and every 3 to 5 years for office personnel and managers. The testing includes blood and urine analysis. At this time no First Solar employee has tested above cadmium blood or urine action levels due to occupational exposure.

### **4.2 Process and equipment improvements**

#### **4.2.1 Edge delete**

The current edge-delete process consists of sandblasting the outer 1 cm of the module to remove the semiconductors and electrode materials. Edge delete prevents shunting of the module at the edges and assists in the encapsulation process. By redesigning the sand-blast-mask clamping system, film undercutting was decreased, thereby improving the shunt resistance of modules. Increasing exhaust airflow improved dust collection and thereby improved operator safety.

Research was also done on grinding as a new method of edge deletion. Grinding would have the advantages of reduced hazardous waste and improved operator safety. Several wheels from 3M were tried and some were found to be capable of removing the semiconductor layers.

#### **4.2.2 CdS material preparation system**

For conditioning of the CdS material for the feeders of the vapor transport system, the procedure that was used involved grinding the sintered CdS by hand with a mortar and pestle and then sifting it with a gyrating sieve shaker. The addition of two pieces of equipment during Phase I greatly improved this procedure. The grinding is now done in a mini-jaw crusher and the sifting is now done with a “controlled-g” sieve shaker. The shaker has an up/down motion with adjustable amplitude and a gasketed lid. Both of these new devices reduce operator exposure to Cd, increase throughput, provide higher quality CdS, and reduce CdS waste. All semiconductor sieving and milling operations are done in chemical hood equipped with HEPA final filtration.

#### **4.2.3 Waste compactor**

Hazardous waste generated at First Solar is regulated by the pounds of waste generated each month. The volume generated each month determines the cost of disposal of the hazardous waste. The cost of disposal of the hazardous waste is determined by the volume generated each month. Introduction of the HazPax hazardous waste compactor has achieved a 112% increase in pounds of waste shipped per drum, a cost savings of \$2.95 per pound, and a waste reduction of 16.7 drums per year. At a cost of \$15 per fiber drum and a shipping cost of \$360 per drum, First Solar has saved an estimated \$573/month with the purchase of the HazPax.

#### **4.2.4 CdCl<sub>2</sub> vapor collection**

Air sampling of the “bell jar” sintering process (directly above the vacuum pump) during a standard run detected 3.3 µg/m<sup>3</sup> of cadmium for 520 minutes of sampling time (or an 8 hour time weighted average of 3.6 µg/m<sup>3</sup>). The detected cadmium was below the permissible exposure limit of 5.0 µg/m<sup>3</sup> during an eight-hour shift. However, a cold trap was ordered and installed to eliminate the exposure from this process.

#### **4.2.5 Wastewater treatment system**

A new wastewater treatment system was installed at the pilot-production facility which allows the manufacturing process to generate 250 gallons of wastewater before a chemical precipitation is necessary, thus requiring only one treatment per shift. The system replaces the 55 gallon system that made 3 to 4 treatments per shift necessary. The effluent discharge still meets the regulatory limit of less than 0.3 PPM for cadmium. The new treatment system also includes filter pressing of the sludge generated from the precipitation process, thus minimizing the volume of this non-hazardous waste.

## Summary and Plans

Principle achievements during Phase I include the following:

- Produced over 6200 8ft<sup>2</sup> CdS/CdTe plates
- Implemented five new diagnostic and quality control systems, including automated CdS thickness and CdTe pinhole number-density mapping systems.
- Demonstrated improved CdTe-thickness uniformity. From a population of more than 1100 plates, the mean standard deviation within a plate was 7.3% and the standard deviation of individual-plate averages was 6.8%.
- Developed new laser-scribing and encapsulation processes.
- Completed construction and began testing of a large vapor-CdCl<sub>2</sub> chamber.
- Designed and began construction of a system capable of depositing CdS and CdTe on 1,500,000 8ft<sup>2</sup> plates/year.
- Researched the effect of buffer and CdS layers on device performance and stability. A cell with 13.9% efficiency on a high-quality substrate and a cell with 12.4% efficiency without a CdS layer were produced.
- Demonstrated plasma cleaning as a viable pre-contact cleaning approach.
- Developed 3 pieces of equipment to perform research: a module-sized sputter system, a small-area vapor-CdCl<sub>2</sub> system, and small-area vapor-transport system.
- Characterized the temperature dependence of CdTe modules.
- Used contactless measurement of V<sub>oc</sub> and photoluminescence to gain insight into the effect of Cu on CdTe devices.
- Completed first round of accelerated-life-testing. Changes in stability performance were correlated with back-contact and other processing variables.
- Demonstrated field stability with a thorough review of field performance for periods up to 5 years.
- Conducted a comprehensive emissions survey.
- Implemented process improvements in edge delete, CdS material preparation, waste compaction, CdCl<sub>2</sub>-vapor collection and wastewater treatment which resulting in reduced costs, reduced emissions, and improved operator safety.

Plans for Phase II include the following:

- Bring the “100MW” coater (the high-speed, 4ft-web, CdS/CdTe deposition system) on line. Use the system to improve deposition uniformity, reproducibility, and material utilization.
- Improve high-throughput laser and encapsulation processes.
- Construct temperature- and ambient-controlled light-soak stations and use the stations for a 2<sup>nd</sup> round of accelerated life testing.
- Research buffer layers and alternative contacts on small and module scale.
- Advance understanding of device operation through characterization and analysis. This activity will include enhancement of spectral-response measurement and SEM/EDS systems.
- Provide modules utilizing all-dry back contacts for field tests.
- Demonstrate improved module (60cm x 120cm) efficiency through the use of thin CdS and buffer layers.

## Appendix: February 1999 Emissions Study

A comprehensive emissions survey of the First Solar pilot-production facility was conducted in February 1999. The results are summarized in section 4.1.1 of this report. The details of the survey follow:

### Sintering of cadmium sulfide material

The CdS source material currently being purchased from an outside vendor does not match the requirements of the powder feeders currently employed in the vapor deposition system. The sintering process (a process whereby the bulk material is partially melted, and consolidates into a larger mass) helps to eliminate this problem. Seventy percent of the sintered source material meets the size requirements for the current feeders on the deposition system (LDS). Thirty percent of the material is too small in size and is currently stored for R&D use.

Process	Source CdS	Source Cd	Total Cd Emissions	Solids/ Other Emissions**
Current (20)	142 g	111g	2.44 g	0.024 g / 2.42 g
*Current - batch	710 g	555 g	12.2 g	0.12 g / 12.1 g
Max (360)	2.56 kg	2.0 kg	44g	0.44 g / 43.56 g

\*The current data is the amount of CdS material sintered for 20 plates per day however, this would be impractical so the current process involves one sintering process per week, generating enough material for one week.

\*\*Solids emissions = cadmium chloride solid crystals currently disposed of as a hazardous material. Other emissions = Cd particles bonding to the sintering chamber, particles filtered by the vacuum pump oil, and particles emitted to the air.

*Emissions qualification:* mass balance calculations.

### Large Deposition System (LDS)

This process involves the deposition of the semiconductor materials (cadmium sulfide and cadmium telluride) onto a 60 x 120 cm glass substrate in a vacuum chamber. Approximately half of the source material is deposited onto the glass substrate with the majority (94%) providing the semiconductor film and (6%) depositing on the “sunny side” of the module which will be removed in a later process.

Process	Source CdS + CdTe	Source Cd	Total Cd Emissions	Solid / Air Emissions
Current (20)	635.6g	331 g	171.4g	171g / .023 mg
Maximum (360)	11.45 kg	5.96 kg	3.1 kg	3.1 kg / 0.7mg

Solid emission = Cd deposited on vacuum chamber walls, on pipes, and in vacuum pump oil. Air emission = Cd vented to outside environment. Operator exposure = 0.38  $\mu\text{g}/\text{m}^3$  for 8 hr TWA (Normalized)

*Emission Qualification:* For the solid emissions, mass balance calculation were used with assistance of the Beta Back Scatter instrument to evaluate film thickness of deposited films and to measure Cd deposited on the “ sunny side” of the module, see Appendix II, for this data. Air emissions were estimated using data from an existing Emission

Source Test Report generated by Foley Occupational Environmental and Health Consultants in 1991. Operator exposure is the results of personal air monitoring of an eight-hour work day in which 56 substrates were coated.

Cadmium Chloride Process

This process involves a wet chemical process in which a saturated solution of CdCl<sub>2</sub> in MeOH is applied to the module.

Process	Source MeOH	Total Emissions	Air Emissions
Current (20)	3.54 kg	3.54 kg	3.54 kg
Maximum (360)	63.74 kg	63.74 kg	63.74 kg

Air emissions = methanol vented to outside environment.

*Emission Qualification:* Mass balance calculations assuming MeOH 100% volatile.

Cadmium Chloride “Cold Hot Cold Rinse”

This process involves the rinsing of the module with cold then hot then cold water to remove CdCl<sub>2</sub> crystals that formed during the cadmium chloride process.

Process	Wastewater Generated	Total Cd Emissions	Water Cd Emissions
Current (20)	20 gallons	15.0 g	15.0g
Maximum (360)	360 gallons	269.8 g	269.8 g

Water Emissions = wastewater pumped to the wastewater treatment system.

*Emission Qualification:* Laboratory results from Jones and Henry Lab.

Buffing Process

This process involves removal of deposited film from the “sunny side” of the module.

Process	CdTe + CdS Mat'l Removed	Total Cd Emissions	Cd Solid + Air Emissions	Air VOC's (buffing comp.)
Current (20)	23.91g	11.8 g	11.8 g	666 g
Maximum (360)	430 g	213.4 g	213.4 g	12 kg

Solid emission = Cd removed with buffing wheel and buffing compound. Because the Cd is removed with this wet buffing compound, it is assumed that there is negligible Cd in air emissions. The solid material is disposed of as a hazardous material.

Air emission = A down draft ventilation table with a filter is operational in the buffing room. The amount of air emission versus solids emission is not known at this time. The filters are disposed of as a solid hazardous material.

Air VOC's (volatile organic compounds) are from the buffing compound. Planned process improvements are expected to reduce these emissions.

*Emission Qualification:* mass balance calculations were used for the total emission results. The Beta Back Scatter instrument was used to evaluate the film thickness of the deposited Cd on the “sunny side” of the module, see Appendix II for data. Calculations consisted of a module rating of “fair” and 70% coverage.

### Edge Deletion Process

This process consists of sandblasting the outer 1cm area of the module to remove the semiconductors and electrode materials.

Process	CdTe + CdS Mat'l Removed	Total Cd Emissions	Cd Solid + Air Emissions	Sand generation
Current (20)	16.4 g	7.98 g	7.98 g	4.1 kg
Maximum (360)	295 g	143.64 g	143.64 g	74.5 kg

Solid emissions = Cd removed with a sandblaster. The Cd contaminated Al oxide sand is disposed of as a hazardous material.

Air emissions = A down draft ventilation table with a filter is operational in the edge delete room. The amount of air versus solid emission is not known at this time. Air filters are disposed of as a solid hazardous material.

*Emission Qualification:* mass balance calculations used for the total emission results. The Beta Back Scatter system was used to evaluate Cd on module film side.

### Isopropanol Rinse

This rinse is used to remove the excess sand which may be present on the module film after the edge delete process. Note: this step was eliminated after the emissions review (experiments showed that the rinse was detrimental to module efficiency).

Process	Source IPA	Total Emissions	Air Emissions
Current (20)	9.5 kg	9.5 kg	9.5 kg
Maximum (360)	171.6 kg	171.6 kg	171.6 kg

Air emissions = Isopropanol vented to outside environment.

*Emission Qualification:* mass balance calculations assuming IPA 100% volatile.

### Interfacial layer process (Wet Lab)

Process	Wastewater Generated	Total Cd Emissions	Water Cd Emission
Current (20)	100 gallons	4.09 g	4.09 g
Maximum (360)	1800 gallons	73.6 g	73.6 g

Water Emissions = wastewater pumped to wastewater treatment system.

*Emission Qualification:* analysis by Jones and Henry Lab.

### Back contact etchant

Process involves the submersion of the module in an etchant.

Process	Waste Etchant	Total Cd Emissions	Water Cd Emissions
Current (20)	50 gallons	0.05 g	0.05 g
Maximum (360)	900 gallons	0.9 g	0.9 g

Water Emissions = wastewater pumped to wastewater treatment system.

*Emission Qualification:* analysis by Jones and Henry Lab.



Laser Scribes #1,#2 and #3

	Process	CdTe + CdS Material Removed	Total Cd Emissions	Cd Air + Solid Emissions
Scribe #1	Current (20)	14.2 g	6.7 g	6.7g
Scribe #1	Maximum (360)	256 g	121 g	121 g
Scribe #2	Current (20)	12.9 g	6.1 g	6.1 g
Scribe #2	Maximum (360)	233 g	109 g	109 g
Scribe #3	Current (20)	10.1 g	4.7 g	4.7 g
Scribe #3	Maximum (360)	181 g	85 g	85 g

Air + Solid emissions = Solids collected through HEPA filtration.

*Emission Qualification* = mass balance calculations using the Bata Back Scatter instrument to evaluate film thickness

Wastewater Treatment System

The wastewater treatment system is a collection and treatment of effluent generated from the following processes; “Cold Hot Cold”, and wet process treatments. The wastewater is then treated with lime and polymer (standard precipitation procedures).

Process	Gallons	Cd Water/Solids Emissions
Current (20)	150 gallons per day	0.06 g
Maximum (360)	2700 gallons per day	1.08 g
Sludge current/maximum	5 gallons / 90 gal (approx.)	3.95 g/ 5 gallon

Water emissions = Cd in the effluent released to the environment.

Solid emissions = Cd in the precipitation sludge. Disposal as a non-regulated waste in a regulated landfill (sludge passes TCLP).

*Emission Qualification:* analysis by Jones & Henry Lab.

Recycling Process

Recycling of off-specification, broken pates and modules. This process consists of removing the semiconductor material from the glass substrate and precipitating the Cd into a sludge solid. The glass is then sent to a recycling vendor and the Cd sludge is disposed of as a solid waste.

Process	Etched glass	Cd Removed	Final Effluent Emissions	Final Solids Emissions
Current	50 module/plates	400 grams	0.05 g	395.95 g
Maximum	150 module/plates	1200 grams	0.15 g	1199.85 g

Effluent = Supernatant from treated etchant released to the environment.

Solids emissions = Precipitation sludge and glass dust from the milling process (to a hazardous waste landfill).

*Emission Qualifications:* analysis by Jones and Henry Lab.

Summary of predicted emissions (February 1999 survey):

emission	Cd emissions		VOC emissions	
	20 module	360 module	20 modules	360 modules
Air	0.02 mg	0.7 mg	3.5 kg	63.6 kg
Solid	210 g	3.6 kg	0	0
Effluent	419 g	1.6 kg	0	0
Total	629 g	5.2 kg	0	0

VOC = Volatile organic compounds (here = methanol; isopropanol emissions were eliminated as of March 1999).

The air emission of 0.7 mg/day (0.0015 lb/day) of cadmium that is predicted for the 360 module/day line is still well below the limit of 10 lb/day, even without any of the anticipated waste reduction improvements. This low emission will continue to entitle First Solar to “De Minimus” Source Exemption for Cd emissions. Air emissions will be regularly monitored to confirm this status.

The air emission of 63.6 kg/day (140 lb/day) of methanol that is predicted for the 360 module/day line is above the limit of 10 lb/day. If anticipated alternatives currently under investigation, such as aqueous-CdCl<sub>2</sub> or vapor-CdCl<sub>2</sub>, are not successful, permitting will be required.

## Glossary of Abbreviations

AJAI	AJA International
ALT	Accelerated life test
APVCD	Atmospheric-pressure chemical-vapor deposition
CCD	Charge coupled device
CSS	Close-spaced sublimation
Cu <sub>Cd</sub>	Copper on a cadmium site
CW	Continuous wave (laser)
DAP	Donor-acceptor pair
DC	Direct current
EVA	Ethylene vinyl acetate
FF	Fill factor
FSEC	Florida Solar Energy Center
HRT	High-resistance tin oxide
IFL	Interfacial layer
IV	Current-Voltage measurement
IV(T)	IV as a function of temperature
J <sub>L</sub> (V)	Light-induced current as a function of voltage
J <sub>sc</sub>	Short circuit current
LDS	Large deposition system (2' x 4' plates by VTD)
LED	Light emitting diode
LOF	Libbey-Owens Ford
MQT	Qualification test
MWp	Peak megawatts (at standard conditions) of PV produced
NREL	National Renewable Energy Laboratory
OC	Open circuit (bias during stress)
PL	Photoluminescence
PPM	Parts per million
PV	Photovoltaics
PVUSA	Photovoltaics for Utility Scale Applications program
RF	Radio frequency
RL	Resistive load (bias during stress - near maximum power point)
RMS	Small-area (4" x 4") close-spaced sublimation system
R <sub>oc</sub>	Resistance at open circuit (series resistance)
SC	Short circuit (bias during stress)
SWTDI	Southwest Technology Development Institute
TCO	Transparent conducting oxide
TECO	Toledo Edison Company (array)
UV	Ultraviolet
V <sub>Cd</sub>	Cadmium vacancy
V <sub>oc</sub>	Open circuit voltage
VOC	Volatile organic compounds
VTD	Vapor transport deposition
ZTO	Zinc stannate (zinc tin oxide)

## References

- [1] D. A. Cusano, "CdTe solar cells and photovoltaic heterojunctions in II-VI compounds," *Solid State Electronics*, vol. 6, pp. 217-232, 1963.
- [2] C. H. Henry, "Limiting efficiencies of ideal single and multiple energy gap terrestrial solar cells," *J. Appl. Phys.*, vol. 51, pp. 4494-4500, 1980.
- [3] J. Britt and C. Ferekides, "Thin-film CdS/CdTe solar cell with 15.8% efficiency," *Applied Physics Letters*, vol. 62, pp. 2851-2, 1993.
- [4] T. Aramoto, S. Kumazawa, H. Higuchi, T. Arita, S. Shibutani, T. Nishio, J. Nakajima, M. Tsuji, A. Hanafusa, T. Hibino, K. Omura, H. Ohyama, and M. Murozono, "16.0% efficient thin-film CdS/CdTe solar cells," *Japanese Journal of Applied Physics*, vol. 36, pp. 6304-6305, 1997.
- [5] T. L. Chu and S. S. Chu, "Recent progress in thin-film cadmium telluride solar cells," *Progress in Photovoltaics: Research and Applications*, vol. 1, pp. 31-42, 1993.
- [6] B. Kroposki, T. Strand, R. Hansen, R. Powell, and R. Sasala, "Technical evaluation of Solar Cells, Inc., CdTe modules and array at NREL," *Proceedings of the 25th IEEE Photovoltaic Specialists Conference*, pp. 969-972, 1996.
- [7] S. Ikegami, "CdS/CdTe solar cells by the screen-printing sintering technique: fabrication, photovoltaic properties and applications," *Solar Cells*, vol. 23, pp. 89-105, 1988.
- [8] P. Moskowitz, "Environmental, health and safety issues related to the production and use of CdTe photovoltaic modules," *Int. J. Solar Energy*, vol. 12, pp. 259-281, 1992.
- [9] M. H. Patterson, A. K. Turner, M. Sadeghi, and R. J. Marshall, "Health, safety and environmental aspects of the use of cadmium compounds in thin film PV modules," *Solar Energy Materials and Solar Cells*, vol. 35, pp. 305-310, 1994.
- [10] R. Sasala and T. Zhou, "Environmentally responsible production, use and disposition of Cd-Bearing PV modules," *IEEE First World Conference on Photovoltaic Energy Conversion*, vol. 1, pp. 311-4, 1994.
- [11] J. Bohland, T. Dapkus, K. Kamm, and K. Smiegielski, "Photovoltaics as hazardous materials: the recycling solution," *Proceedings of the 2nd IEEE World Photovoltaic Specialists Conference*, pp. 716-719, 1998.
- [12] R. C. Powell, U. Jayamaha, G. L. Dorer, and H. McMaster, "Scaling and qualifying CdTe/CdS module production," *15th NCPV Photovoltaics Program Review, AIP Conference Proceedings No. 462*, pp. 31-36, 1998.
- [13] B. E. McCandless and R. W. Birkmire, "Influence of processing conditions on performance and stability in polycrystalline thin-film CdTe-based solar cells," *15th NCPV Photovoltaics Program Review, AIP Conference Proceedings No. 462*, pp. 182-187, 1998.
- [14] X. Wu, P. Sheldon, Y. Mahathongdy, R. Ribelin, A. Mason, H. R. Moutinho, and T. J. Coutts, "CdS/CdTe thin-film solar cells with a zinc stannate buffer layer," *15th NCPV Photovoltaics Program Review, AIP Conference Proceedings No. 462*, pp. 37-41, 1998.

- [15] X. Li, R. Ribelin, Y. Mahathongdy, D. Albin, R. Dhere, D. Rose, S. Asher, H. Moutinho, and P. Sheldon, "The effect of high-resistance SnO<sub>2</sub> on CdS/CdTe device performance," *NCPV Photovoltaics Program Review- Proceedings of the 15th Conference*, vol. 462, pp. 230-235, 1998.
- [16] D. H. Rose, "The effect of oxygen on CdTe-absorber solar cells deposited by close-spaced sublimation," in *Electrical and Computer Engineering*. Boulder, CO: University of Colorado, 1997, pp. 198.
- [17] D. Albin, D. Rose, R. Dhere, D. Niles, A. Swartzlander, A. Mason, D. Levi, H. Moutinho, and P. Sheldon, "Tin oxide stability effects - their identification, dependence on processing and impacts on CdTe/CdS solar cell performance," *AIP Proceedings No. 394, 14th NREL/SNL Photovoltaics Program Review*, pp. 665-681, 1996.
- [18] T. Coutts, X. Wu, P. Sheldon, and D. Rose, "Development of high-performance transparent conducting oxides and their impact on the performance of CdS/CdTe solar cells," *Proceedings of the 2nd IEEE World Photovoltaic Specialists Conference*, pp. 721-723, 1998.
- [19] F. A. Abou-Elfotouh, H. R. Moutinho, F. S. Hasoon, R. K. Ahrenkiel, D. Levi, and L. L. Kazmerski, "Effects of processing on the properties of polycrystalline CdTe grown by various deposition techniques," *Proceedings of the 23rd IEEE Photovoltaic Specialists Conference*, pp. 491-4, 1993.
- [20] R. W. Birkmire, J. E. Phillips, W. N. Shafarman, S. S. Hegedus, and T. A. Yokimcus, "Polycrystalline thin film materials and devices," Institute of Energy Conversion, Newark, DE, Final report to NREL under subcontract XN-0-101123-1, March 1993.
- [21] D. Niles, X. Li, P. Sheldon, and H. Höchst, "A photoemission determination of the band diagram of the Te/CdTe interface," *J. Appl. Phys.*, vol. 77, pp. 1-5, 1995.
- [22] D. W. Niles, X. Li, D. Albin, D. Rose, T. Gessert, and P. Sheldon, "Evaporated Te on CdTe: a vacuum-compatible approach to making back contact to CdTe solar cell devices," *Progress in Photovoltaics: Research and Applications*, vol. 4, pp. 225-229, 1996.
- [23] D. Grecu and A. D. Compaan, "Photoluminescence study of Cu diffusion in CdTe," *15th NCPV Photovoltaics Program Review, AIP Conference Proceedings No. 462*, pp. 224-229, 1998.
- [24] D. Grecu and A. D. Compaan, "Photoluminescence study of Cu diffusion and electromigration in CdTe", *Applied Physics Letters*, vol. 75, pp. 361, 1999.
- [25] D. Grecu, Ph.D. dissertation in Physics: University of Toledo, 1999 (unpublished).
- [26] R. W. Birkmire, J. E. Phillips, W. A. Buchanan, S. S. Hegedus, B. E. McCandless, W. N. Shafarman, and T. A. Yokimcus, "Processing & modeling issues for thin film solar cell devices," Institute of Energy Conversion, Newark, DE, Annual report to NREL under subcontract X-AV-13170-01, March 1994.
- [27] N. Romeo, A. Bosio, R. Tedeschi, and V. Canevari, "High efficiency and stable CdTe/CdS thin film solar cells on soda lime glass," *2nd World Conference on Photovoltaic Solar Energy Conversion*, pp. 446-7, 1998.

REPORT DOCUMENTATION PAGE			Form Approved OMB NO. 0704-0188	
Public reporting burden for this collection of information is estimated to average 1 hour per response, including the time for reviewing instructions, searching existing data sources, gathering and maintaining the data needed, and completing and reviewing the collection of information. Send comments regarding this burden estimate or any other aspect of this collection of information, including suggestions for reducing this burden, to Washington Headquarters Services, Directorate for Information Operations and Reports, 1215 Jefferson Davis Highway, Suite 1204, Arlington, VA 22202-4302, and to the Office of Management and Budget, Paperwork Reduction Project (0704-0188), Washington, DC 20503.				
1. AGENCY USE ONLY (Leave blank)	2. REPORT DATE October 1999	3. REPORT TYPE AND DATES COVERED Annual Technical Report, Phase I, 1 April 1998 – 31 March 1999		
4. TITLE AND SUBTITLE Technology Support for High-Throughput Processing of Thin-Film CdTe PV Modules; Annual Technical Report, Phase I, 1 April 1998 – 31 March 1999			5. FUNDING NUMBERS C: ZAK-8-17619-17 TA: PV905001	
6. AUTHOR(S) D.H. Rose, R.C. Powell, D. Grecu, U. Jayamaha, J.J. Hanak, J. Bohland, K. Smigielski, and G.L. Dorer				
7. PERFORMING ORGANIZATION NAME(S) AND ADDRESS(ES) First Solar, L.L.C. Research Center 12900 Eckel Junction Road Perrysburg, OH 43551			8. PERFORMING ORGANIZATION REPORT NUMBER	
9. SPONSORING/MONITORING AGENCY NAME(S) AND ADDRESS(ES) National Renewable Energy Laboratory 1617 Cole Blvd. Golden, CO 80401-3393			10. SPONSORING/MONITORING AGENCY REPORT NUMBER SR-520-27149	
11. SUPPLEMENTARY NOTES NREL Technical Monitor: H.S. Ullal				
12a. DISTRIBUTION/AVAILABILITY STATEMENT National Technical Information Service U.S. Department of Commerce 5285 Port Royal Road Springfield, VA 22161			12b. DISTRIBUTION CODE	
13. ABSTRACT ( <i>Maximum 200 words</i> ) This report describes work performed by First Solar, L.L.C., during Phase I of this 3-year subcontract. The research effort of this subcontract is divided into four areas: 1) process and equipment development, 2) efficiency improvement, 3) characterization and analysis, and 4) environmental, health, and safety. As part of the process development effort, the output of the pilot-production facility was increased. More than 6200 8-ft <sup>2</sup> CdS/CdTe plates were produced during Phase I -- more than double the total number produced prior to Phase I. This increase in pilot-production rate was accomplished without a loss in the PV conversion efficiency: the average total-area AM1.5 efficiency of sub-modules produced during the reporting period was 6.4%. Several measurement techniques, such as large-area measurement of CdS thickness, were developed to aid process improvement, and the vapor-transport deposition method was refined. CdTe thickness uniformity and reproducibility were improved. From a population of more than 1100 plates, the mean standard deviation within a plate was 7.3% and the standard deviation of individual-plate averages was 6.8%. As part of the efficiency-improvement task, research was done on devices with thin-CdS and buffer layers. A cell with 13.9% efficiency was produced on a high-quality substrate, and higher than 12% efficiency was achieved with a cell with no CdS layer. A number of experiments were performed as part of the characterization and analysis task. The temperature dependence of CdTe modules was investigated; the power output was found to be relatively insensitive (<5%) to temperature in the 25° to 50°C range. As part of the characterization and analysis task, considerable effort was also given to reliability verification and improvement. The most carefully monitored array, located at the NREL, was found to have unchanged power output within the margin of error of measurement (5%) after 5 years in the field. The first round of National CdTe Team stability tests were concluded. One back-contact formulation resulted in cells that increased in efficiency as a result of 9700 hours of light soaking. As part of the environmental, health, and safety task, an emissions survey was performed for the pilot-production facility. For production of 360 modules/day, it was predicted that the cadmium emissions would be only 0.015% of the level that would require any permitting; however, methanol emissions may require permitting if anticipated process changes are not implemented. Process improvements in edge delete, CdS material preparation, waste compaction, CdCl <sub>2</sub> -vapor collection, and wastewater treatment were made, resulting in reduced costs, reduced emissions, and improved operator safety.				
14. SUBJECT TERMS photovoltaics ; Thin-Film Photovoltaic Partnership ; CdS ; CdTe ; high-throughput processing			15. NUMBER OF PAGES	
			16. PRICE CODE	
17. SECURITY CLASSIFICATION OF REPORT Unclassified	18. SECURITY CLASSIFICATION OF THIS PAGE Unclassified	19. SECURITY CLASSIFICATION OF ABSTRACT Unclassified	20. LIMITATION OF ABSTRACT UL	